Ecophysiological responses of Ostreopsis towards temperature: A case study of benthic HAB facing ocean warming

Kevin Drouet, Rodolphe Lemée, Emilie Guilloud, Sophie Schmitt, A. Laza-Martinez, S. Seoane, Marc Boutoute, Damien Réveillon, F. Hervé, Raffaele Siano, et al.

Editor: Dr Po Teen Lim

Journal Pre-proof

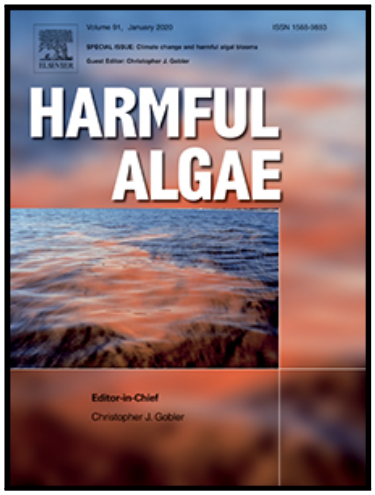

Ecophysiological responses of Ostreopsis towards temperature: a case study of benthic HAB facing ocean warming

K. Drouet , R. Lemée , E. Guilloud , S. Schmitt ,
A. Laza-Martinez , S. Seoane , M. Boutoute , D. Réveillon ,
F. Hervé , R. Siano , C. Jauzein

PII: S1568-9883(24)00082-9
DOI: https://doi.org/10.1016/j.hal.2024.102648
Reference: HARALG 102648

To appear in: *Harmful Algae*

Received date: 3 November 2023
Revised date: 5 April 2024
Accepted date: 15 May 2024

Please cite this article as: K. Drouet , R. Lemée , E. Guilloud , S. Schmitt , A. Laza-Martinez , S. Seoane , M. Boutoute , D. Réveillon , F. Hervé , R. Siano , C. Jauzein , Ecophysiological responses of Ostreopsis towards temperature: a case study of benthic HAB facing ocean warming, *Harmful Algae* (2024), doi: https://doi.org/10.1016/j.hal.2024.102648

Ecophysiological responses of *Ostreopsis* towards temperature: a case study of benthic HAB facing ocean warming

K. Drouet[1,2*], R. Lemée[1], E. Guilloud[2], S. Schmitt[2], A. Laza-Martinez[3,4], S. Seoane[3,4], M. Boutoute[1], D. Réveillon[5], F. Hervé[5], R. Siano[2] and C. Jauzein[2]

1 Sorbonne Université, CNRS - Laboratoire d'Océanographie de Villefranche (UMR 7093) – Villefranche-sur-Mer 06230, France

2 Ifremer, DYNECO/Pelagos – F-29280 Plouzané, France

3 Department of Plant Biology and Ecology - University of the Basque Country UPV/EHU – Leioa 48940, Spain

4 Research Centre for Experimental Marine Biology and Biotechnology (Plentzia Marine Station, PiE-UPV/EHU) – Plentzia 48620, Spain

5 Ifremer, PHYTOX, Laboratoire METALG, F-44000 Nantes, France

*Corresponding author: kevindrouet83@gmail.com

Running title: *Ostreopsis* eco-physiological responses towards temperature

Highlights:

- *O.* cf. *siamensis* had a colder and shorter thermal niche than *O.* cf. *ovata*.
- Some clones of *O.* cf. *siamensis* have a fast growing strategy, not *O.* cf. *ovata*.
- Acclimation to temperature relies on xanthophyll cycle pigments or lipid content.
- Toxicity decreases with low temperatures and is maximal under optimal growth ones.
- When both species are present, the toxic risk may increase with the global warming.

Abstract:

Reports of the benthic dinoflagellate *Ostreopsis* spp. have been increasing in the last decades, especially in temperate areas. In a context of global warming, evidences of the effects of increasing sea temperatures on its physiology and its distribution are still lacking and need to be investigated. In this study, the influence of temperature on growth, ecophysiology and toxicity was assessed for several strains of *O.* cf. *siamensis* from the Bay of Biscay (NE Atlantic) and *O.* cf. *ovata* from NW Mediterranean Sea. Cultures were acclimated to temperatures ranging from 14.5 °C to 32 °C in order to study the whole range of each strain-

specific thermal niche. Acclimation was successful for temperatures ranging from 14.5 °C to 25 °C for *O.* cf. *siamensis* and from 19 °C to 32 °C for *O.* cf. *ovata,* with the highest growth rates measured at 22 °C (0.54 – 1.06 d^{-1}) and 28 °C (0.52 – 0.75 d^{-1}), respectively. The analysis of cellular content of pigments and lipids revealed some aspects of thermal acclimation processes in *Ostreopsis* cells. Specific capacities of *O.* cf. *siamensis* to cope with stress of cold temperatures were linked with the activation of a xanthophyll cycle based on diadinoxanthin. Lipids (neutral reserve lipids and polar ones) also revealed species-specific variations, with increases in cellular content noted under extreme temperature conditions. Variations in toxicity were assessed through the *Artemia franciscana* bioassay. For both species, a decrease in toxicity was observed when temperature dropped under the optimal temperature for growth. No PLTX-like compounds were detected in *O.* cf. *siamensis* strains. Thus, the main part of the lethal effect observed on *A. franciscana* was dependent on currently unknown compounds. From a multiclonal approach, this work allowed for defining specificities in the thermal niche and acclimation strategies of *O.* cf. *siamensis* and *O.* cf. *ovata* towards temperature. Potential impacts of climate change on the toxic risk associated with *Ostreopsis* blooms in both NW Mediterranean Sea and NE Atlantic coast is further discussed, taking into account variations in the geographic distribution, growth abilities and toxicity of each species.

Key-words: Temperature; Acclimation; Harmful Algal Blooms; *Ostreopsis*; Benthic dinoflagellate; Growth; Toxicity

1. Introduction

Among microalgae species responsible for harmful algal bloom development, the harmful benthic dinoflagellate genus *Ostreopsis* represents an emerging threat for human health. Blooms of this genus have mainly been observed in temperate areas (Shears and Ross, 2009; Rhodes, 2011; Selina *et al.*, 2014), and especially in the Mediterranean Sea (Mangialajo *et al.*, 2011; Blanfuné *et al.*, 2015; Accoroni and Totti, 2016). To date, twelve *Ostreopsis* species have been identified and characterized (Verma *et al.*, 2023). The description of *Ostreopsis* species was traditionally based upon morphological features, but the high degree of morphological plasticity within and among species made the genetic identification mandatory for the proper identification and characterization of species, as well as for inter-comparison of species-specific studies (Parsons *et al.*, 2012; Chomérat *et al.*, 2019; Chomérat *et al.*, 2020).

For instance, *O. siamensis* and *O. ovata* were described for the first time only based on morphological features and were not genetically characterized. Thus, species morphologically associated with these two taxa are now referred as *O.* cf. *siamensis* and *O.* cf. *ovata*, respectively.

Blooming episodes formed by certain species of *Ostreopsis* might result in toxic outbreaks affecting human health through skin irritations induced by direct contact (Tichadou *et al.*, 2010; Tubaro *et al.*, 2011) or through serious respiratory symptoms caused by aerosol inhalation (Durando *et al.*, 2007; Illoul *et al.*, 2012; Vila *et al.*, 2016). Apart from human health, *Ostreopsis* spp. also exhibit allelopathic effects on marine fauna (Pavaux *et al.*, 2019, 2020a, 2020b). *Ostreopsis* cf. *ovata* is known to produce a high diversity of palytoxin analogs such as ovatoxins, ostreocins and mascarenotoxins (Pavaux *et al.*, 2020a). Concerning *O.* cf. *siamensis*, traces of palytoxin-like compounds as well as ostreocins have only been found in strains from Pacific and Asia (Verma *et al.*, 2016; Chomérat *et al.*, 2020), but not in strains from Atlantic or Mediterranean Sea (Ciminiello *et al.*, 2013). However, toxicity bioassays based on cell lines viability (Cagide *et al.*, 2009) and mortality of invertebrate organisms (Laza-Martinez *et al.*, 2011) revealed active toxicity in these Atlantic strains, suggesting that other non-identified allelopathic compounds could be responsible for *O.* cf. *siamensis* toxicity.

The development of *Ostreopsis* species and their blooms phenology is known to be driven by an assembly of biotic and abiotic factors influencing physiological mechanisms and growth ability. Environmental parameters such as hydrodynamics, biotic substratum, irradiance, salinity, nutrients availability and sea temperature are suggested to be the most influencing factors (Parsons *et al.*, 2012; Accoroni and Totti, 2016). Among these, the temperature can play a major role in both definition of the ecological niche (David *et al.*, 2012; Scalco *et al.*, 2012; Drouet *et al.*, 2021) and the phenology of blooms (Carnicer *et al.*, 2015; Drouet *et al.*, 2022). In both cases, temperature can regulate the presence of the species in the water column by controlling the germination of resting stages (if they are part of the life cycle of the species) (Bravo and Anderson, 1994; Bravo *et al.*, 2012; Accoroni *et al.*, 2014; Fischer *et al.*, 2018) and/or directly influencing their growth (Tian, 2006; Pezzolesi *et al.*, 2012). In temperate areas in particular, *Ostreopsis* spp. blooms are recurrent phenomena that seem to be favoured by high temperatures: they mainly occur during the summer period, with maximal abundances often corresponding to relatively high temperatures, but not necessarily the highest one (Totti *et al.*, 2010; Cohu *et al.*, 2011; Laza-Martinez *et al.*, 2011; Selina *et al.*, 2014; Drouet *et al.*, 2022). Extensive laboratory studies conducted on *O.* cf. *ovata* showed the

highest growth rates of Mediterranean strains at temperatures ranging between 20 °C and 27 °C (Pistocchi *et al.*, 2011; Pezzolesi *et al.*, 2012; Scalco *et al.*, 2012; Gémin *et al.*, 2021), whereas Asian or Brazilian strains exhibited highest growth rates at temperatures ranging from 25 °C to 30 °C (Nascimento *et al.*, 2012; Yamaguchi *et al.*, 2012; Tawong *et al.*, 2015). Such differences in thermal ranges suggest strain-specific variations in the relationship between growth abilities and temperature. They may represent physiological adaptations of cells to the specific environmental conditions of isolation sites that can lead to the emergence of genetically distinct populations called ecotypes. Several studies also reported that temperature influence *Ostreopsis* cell metabolism and specifically, at least for *O.* cf. *ovata*, the toxin content. Previous works report conflicting trends in toxin content varying as a function of temperature (Pezzolesi *et al.*, 2012; Gémin *et al.*, 2021), however, that might also be linked to strain-specific response. It is also still unclear if such temperature effect is either direct on toxin synthesis pathways or indirect through modifications of growth rate.

Anthropic activities might affect HABs development through climate change especially as a consequence of the worldwide increase of sea temperature. For benthic species (including *Ostreopsis* spp.), Tester *et al.* (2020) recently described a potential migration of their distribution from tropical areas towards higher latitudes and an extension of their habitat in temperate areas in response to global warming. In the face of such suspected change, elaborating risk assessment and management for the mitigation of HABs in recreational waters are crucial, taking into account benthic species (Anderson, 2009; Berdalet *et al.*, 2016, 2017). While *O.* cf. *ovata* has been extensively observed and studied in the Mediterranean Sea (Mangialajo *et al.*, 2011; Accoroni and Totti, 2016), a bloom of this toxic species has only been recently reported in the Bay of Biscay (NE Atlantic) (Chomérat *et al.*, 2022). On the other hand, *O.* cf. *siamensis* has been described in the Bay of Biscay, occasionally forming blooms, over the last decade (Laza-Martinez *et al.*, 2011; David *et al.*, 2013; Drouet *et al.*, 2021). As both of these areas are exposed to SST warming (deCastro *et al.*, 2009; Costoya *et al.*, 2015; Pastor *et al.*, 2020), investigations regarding the physiological responses of local HAB species towards increasing temperatures are needed to apprehend a potential expansion of the genus.

Microalgae species have several ways to respond to changes in environmental conditions depending on the timescale. They can sporadically respond to punctual stress (cellular response), or acclimate and even adapt to long-term environmental changes (population response). At the cellular scale, temperature is known to affect the functionalities of enzymes in charge of photosynthesis (Salvucci and Crafts-Brandner, 2004) and can thus

directly influence the photosynthetic activity and ultimately growth of microalgal cells (Ras *et al.*, 2013). Cells can also use mechanisms such as changes in pigment composition (Anning *et al.*, 2001; López-Rosales *et al.*, 2014), lipid content (Thompson *et al.*, 1992b; Ding *et al.*, 2019) and acquisition and release of specific nutrients (Glibert *et al.*, 2016), to generate an acclimation response to stress and optimize growth. In the end, each clone is characterized by specific characteristics associated with growth capacities (e.g. Jauzein *et al.*, 2008) or stress induced pathways. At the population level, species can take advantage of the high genetic diversity observed in the field, and over the development of HABs in particular (Dia *et al.*, 2014): in response to environmental stress, a selection of advantageous genotypes can occur, favouring clones with high fitness.

The aim of this study was to investigate how different strains of *O.* cf. *siamensis* and *O.* cf. *ovata* can acclimate to various temperature levels and to define the influence of temperature on their toxicity. From a 1.5 year-lasting laboratory experiment, growth abilities and physiological acclimation of cells were characterized over a large temperature gradient (14.5 to 32 °C), using strains isolated from the Bay of Biscay (NE Atlantic) and the Bay of Villefranche-sur-Mer (NW Mediterranean Sea). These physiological traits allowed for the definition of strain-specific favourable and optimal temperatures for growth that give crucial information about the thermal niche at the clone level. They also revealed strategies of physiological changes, in terms of pigment and lipid variations, that both *O.* cf. *siamensis* and *O.* cf. *ovata* can use for their response to thermal stress, including the release of toxic compounds.

2. Material and methods

2.1. Culture conditions

2.1.1. *Ostreopsis* strains and maintenance of stock cultures

Strains of *O.* cf. *siamensis* were isolated from five different sites located along the southeastern coast of the Bay of Biscay, North-East Atlantic (Drouet *et al.*, 2021). The geographical repartition of these isolation sites straddled the frontier between Spain and France (Figure 1). Three or four strains of *O.* cf. *siamensis* were used per site, accounting for 17 strains in total (Supplementary Table 1). For *O.* cf. *ovata*, three strains were used (MCCV54, MCCV98 and MCCV99), all originated from the same site of Rochambeau in the bay of Villefranche-sur-Mer (France, North-Western Mediterranean; Figure 1) and obtained from the Mediterranean Culture Collection of Villefranche (MCCV) in the framework of the

European Marine Biological Resource Centre (EMBRC-France, http://www.embrc-france.fr) (Supplementary Table 1). Strains of *O.* cf. *siamensis* and *O.* cf. *ovata* were grown in K medium (Keller *et al.*, 1987) without silicate, using autoclaved and filtered seawater at salinities of 35 and 38, respectively. Stock cultures were maintained at 22 °C, under a 12:12h light/dark cycle with an irradiance intensity of 150-200 µmol photons·m^{-2}·s^{-1} (leds).

2.1.2. Thermal acclimation experiments

Cultures of *Ostreopsis* used for the experiment were grown in 25 cm², 75 cm² and 150 cm² polystyrene culture flasks (TPP® Cell culture flask, Sigma-Aldrich), on the same culture medium and under the same light cycle than stock cultures. All culture transfers were conducted performing a dilution of 1/5 or 1/10 with fresh medium, targeting a starting cell concentration of about 500 cells·mL^{-1}. During the experiment, temperature was the only variable condition and ranged from 14.5 °C to 32 °C. Under the temperature of 22 °C (selected for the maintenance of stock cultures), all the 20 strains were characterized by estimations of growth rate and toxicity using biotests on *Artemia franciscana* (Pavaux *et al.*, 2020b). For all the *O.* cf. *siamensis* clones (17 strains), these analyses were complemented by a chemical characterization of the toxin content. Among the 20 *Ostreopsis* strains, 9 *O.* cf. *siamensis* strains (Z1, Z7 and Z8 from Zierbena; H1, H8 and H10 from Hondarribia; SJL1, SJL2 and SJL3 from Saint-Jean-de-Luz) and 3 *O.* cf. *ovata* strains (MCCV 54, MCCV 98 and MCCV 99 from Rochambeau) were then selected. They were characterized in more details in terms of growth abilities and physiology and gradually acclimated to increasing (25 °C, 28 °C, 30 °C, 32 °C) and decreasing (19 °C, 16 °C, 14.5 °C) levels of temperature until cultures were no longer capable of surviving.

Estimations of growth rates were conducted for every culture except the first cell transfer after a modification of temperature. Additional parameters, based on direct measurements or collection of biomasses, were only estimated on cultures that were considered acclimated, *i.e.* once a stable growth rate was measured over three successive cell transfers (Wood *et al.*, 2005). In the end, these additional measurements were performed 25 days or later after any change of temperature. They were the source of the characterization of growth abilities (maximal growth rate), of potential signs of cellular stress and acclimation to non-optimal growth conditions (profiles of pigments and lipids) and of toxicity using biotests on *A. franciscana*. All these additional parameters were estimated during the exponential phase of growth of the cultures.

For the extreme cold temperature of 14.5 °C, only the *O.* cf. *siamensis* strains Z8, H10 and SJL1 were used; those were the few strains able to acclimate at this temperature. The biomass produced under this condition was quite low and limited some of the sampling and measurements. Every parameter was monitored for Z8 at this temperature, while toxicity and lipids were missing for SJL1, and only growth could be measured for H8. For the highest temperature of 32 °C, only one *O.* cf. *ovata* strain was characterized: MCCV 98, the only one able to acclimate. At 32 °C, growth, toxicity and the pigment profile of cells were monitored, but not lipids.

2.2. Cell abundance and growth rate

Every two or three days, quantification of cell abundance was performed to establish growth curves of the cultures and estimate their growth rates. Cultures were homogenized before the collection of samples. For this, cells from the bottom were re-suspended using a pipette by flushing gently the bottom of the flask with the culture itself, and then, the whole culture was gently agitated. Sub-samples (4 mL) were then collected and immediately fixed with acidic Lugol (2% vol./vol.). They were kept less than three months at room temperature before analysis. Cell quantification was performed in triplicates using either a Utermöhl chamber (Utermöhl, 1958) under an inverted light microscope (AxioVert 135, x100, Zeiss, Oberkochen, Germany) or a Nageotte hemocytometer (Hecht Assistent, Sondheim vor der Rhön, Germany) and a light microscope (Olympus® BX51, x100, Tokyo, Japan), depending on the volume used for observation. Temporal variations of cell counts allowed for identifying successive phases of microalgal growth and estimating growth rates using the following equation:

$$\mu = \frac{\ln N_1 - \ln N_0}{t_1 - t_0}$$

Where μ is the growth rate (d^{-1}) and N_0 and N_1 are the cell abundances ($cell.mL^{-1}$) at time t_0 and t_1 (d). Following this equation, the maximal growth rate (μ_{max}) was specifically calculated over the exponential growth phase as the slope of the linear regression between the natural logarithm of cell concentration and time. Replicated values of μ_{max} were obtained from successive culture transfers that were established when thermal acclimation was reached.

2.3. Estimations of microalgal toxin content and toxicity

The toxin profile of *O.* cf. *ovata* strains from the Mediterranean Sea was previously characterized. For MCCV54 in particular, it showed a total toxin content ranging from 22.5 and 32.8 pg·cell^{-1} with a toxin profile characterized by ovatoxin-a (56 %), -b (15 %), -c (5 %), -d (8 %), -e (4 %), -f (< 1 %) and putative-palytoxin (12 %) (Brissard *et al.*, 2014). Analyses conducted in the present study were complementary to these estimations: chemical analyses were focused on *O.* cf. *siamensis* strains and bio-assays were used for estimating the toxicity of both *O.* cf. *ovata* and *O.* cf. *siamensis* over various temperature conditions.

2.3.1. *Ostreopsis* cf. *siamensis* toxin extraction and analysis

The 17 strains of *O.* cf. *siamensis* isolated from the Atlantic coast were grown at 22 °C in 150 mL of culture medium. Microalgal cells were collected during the exponential phase. Cell pellets harvested by centrifugation (3000 *g* for 10 min) from multiple batches of cultures were pooled for accumulating between 1.3 to 11 million of cells per strain and stored at -80 °C until extraction.

Toxin extraction and analysis were performed according to Chomérat *et al.* (2019) with minor modifications. Briefly, pellets were recovered in 1.5 mL MeOH 50 %, homogenized, sonicated in an ice bath for 10 min, centrifuged and ultrafiltered (0.2 µm, Nanosep MF, Pall, at 10 000 g). Toxin analyses were conducted using three methods using Liquid Chromatography coupled to tandem Mass Spectrometry (LC-MS/MS) that allowed for the detection of two palytoxins (palytoxin and 42-OH palytoxin), 12 ovatoxins (-a to -k) and 7 other palytoxin-like compounds (ostreocin-a, -b, -d and -e1 and mascarenotoxins-a, -b and -c). Quantification was performed relative to the only available standard Palytoxin (Wako Chemicals GmbH, Germany) with a 7-point calibration curve and assuming similar molar responses between the standard and the PLTX-like molecules. The instrument control, data processing and analysis were conducted using Analyst software 1.6.3. Limit of detection and quantification were 20 and 40 ng.mL^{-1} for PLTX standard.

2.3.2. *Artemia franciscana* toxicity bio-assay

The toxicity of *Ostreopsis* strains was assayed for both *O.* cf. *siamensis* and *O.* cf. *ovata* over the whole temperature gradient tested, using the *Artemia franciscana* bio-assay (Pavaux *et al.*, 2020b). Approximately 100 mg of *A. franciscana* cysts (Sep-Art Artemia cysts, Ocean

Nutrition®, Newark, CA, USA) were hatched in 1 L of filtered seawater at salinity 35 and room temperature, under continuous light exposition (100 µmol·m^{-2}·s^{-1}) and a slight aeration. After 40 hours of incubation, *A. franciscana* larvae moulted into metanauplii instars (stages 2-3), considered to be the most sensitive stage regarding ecotoxicological bio-assays (Nunes *et al.*, 2006). Hatched nauplii were separated from remaining cysts by attracting them with light. They were collected close to the surface using a Pasteur Pipette. Incubations were conducted in 12-wells plates (Sarstedt). Each well was filled with 3 mL of filtered seawater and a defined concentration of *Ostreopsis* cells, then five nauplii were transferred per well. Four different concentrations of *O.* cf. *siamensis* and *O.* cf. *ovata* were tested: 0 (for blank values), 4, 40 and 400 cells·mL^{-1}. Three replicated incubations were performed for each *Ostreopsis* concentration, on the same plate. Plates were placed in the dark to reduce nauplii mortality due to their strong positive phototactism and to limit *Ostreopsis* cell division and associated variations of microalgal cell concentrations. Nauplii mortality was measured at 2, 4, 6, 8, 24 and 48 hours of exposure to *Ostreopsis* cells using a binocular magnifier (Olympus® SZX10, x10, Tokyo, Japan). The death of nauplii was validated when no movement or no reaction to a slight stimulation by agitation was observed after 10 seconds.

2.4. Pigment analyses through High-Performance-Liquid-Chromatography (HPLC)

For each strain, 150 mL of culture, corresponding to approximately $1x10^5$ to $6x10^5$ cells in exponential growth phase, were used for characterizing the pigment profile of *Ostreopsis* cells along the temperature gradient. The biomass was collected by filtering the culture on 25 mm GF/F filters (0.7 µm pore size). Filters were immediately stored at -80 °C and kept at this temperature until analysis. Extractions of pigments from filters were performed in the dark. Filters were placed into glass test tubes and 3 mL of a mix solution (internal standard, composed of methanol and tocopherol) was added. Tubes were vortexed and placed at -20 °C during 30 minutes, sonicated for 10 seconds (20 % amplitude) then placed again at -20 °C for 30 minutes. Extracts were vortexed and filtered through 25 mm diameter Polyvinylidene fluoride (PVDF) syringe filters (45 µm) for cellular debris removal. Then, 500 µL of filtrate were added to 500 µL of tetrabutylammonium acetate (TBAA) buffer in 2 mL amber tubes and vortexed (Mantoura and Llewellyn, 1983). Final extracts were analysed through HPLC using an Agilent HPLC-1100 (Agilent Technologies, Santa-Clara, CA, USA) coupled to the

automatic sample changer Agilent 1260 infinity, according to Van Heukelem and Thomas (2001). Optical densities for solvent (blank, 70% methanol – 30% TBAA) and extracts were measured for a large diversity of pigments, including chlorophyll related (Chlorophyll *a* (Chl *a*), Chlorophyll *b*, Chlorophyll *c2*, Chlorophyll *c2-MGDG*, Chlorophyll *c3*, Chlorophyllide *a*, Chlorophyllide *b* and Divinyl Chlorophyll *a*), carotenoid (Alloxanthin, Antheraxanthin, Astaxanthin, Beta-carotene, Canthaxanthin, Diadinoxanthin (Dd), Diatoxanthin (Dt), Dinoxanthin, Fucoxanthin, 19'-but-fucoxanthin, 19'-hex fucoxanthin, Lutein, Neoxanthin, Peridinin, Pheophytin *a*, Pheophorbide *a*, Prasinoxanthin, Violaxanthin, and Zeaxanthin) and Mixed pigments MIX-1 (DHI standard) pigments. Pigment concentrations were estimated using standard curves determined for each pigment.

In order to scale the xanthophyll cycle pigments to the total amount of Chl *a*, concentrations of Dd, Dt and the total pool Dd+Dt were normalized by Chl *a* concentrations. The xanthophyll de-epoxydation state (DES) was calculated as Dt/(Dd+Dt), indicating the proportion of Dt, the de-epoxydized form of Dd, regarding to the total pool of xanthophyll cycle pigments. Similarly, the epoxidation state (ES) was calculated as Dd/(Dd+Dt).

2.5. Lipid composition

150 mL of culture of each strain were centrifuged (3000 g, 10 minutes) and stored at -80 °C to obtain cell pellets (between 1.1 and 14.1 x10^6 cells depending on the strain and the condition of temperature) from which lipids were extracted according to the Bligh and Dyer (1959) method. The lipid methylation was performed according to Morrison and Smith (1964). Pellets were recovered in a solvent mixture of methanol/chloroform/water + NaCl 0.7 % (2/1/0.8 vol./vol./vol.) and extracted twice using a Mixer Mill MM400 (Retsh, Haan, Germany). Phases of the solvent mixture were then separated overnight by addition of chloroform and water + NaCl 0.7% for a final solvent ratio of methanol/chloroform/water + NaCl 0.7 % of 2/2/1.8 (vol./vol./vol.). The solvents were evaporated using a rotatory evaporator and extracted lipids were weighed in tarred vials for total lipids content evaluation. Lipid classes isolations were carried out by thin layer chromatography (TLC Silica gel 60 F254, 20 x 20 cm, Merck, Darmstadt, Germany) and lipids were visualized under UV (240 and 360 nm) using dichlorofluorescein 0.2 % (in ethanol). Neutral lipids, glycolipids and phospholipids were separated using Hexane/ether/acetic acid 170/30/2 (vol./vol./vol.), chloroform/methanol/water 70/30/4 (vol./vol./vol.) and chloroform/methanol/ammonia

50/50/5 (vol./vol./vol.), respectively. Lipids classes were then quantified using a Iatroscan MK5 (Iatron, Tokyo, Japan) and Chromarods S5.

2.6. Statistical analysis and modelling

In this study, differences in growth rates, toxicity, pigment and lipid amounts among *Ostreopsis* strains under the different temperatures tested were assessed using non-parametric tests (Kruskal-Wallis and Friedman ANOVAs) after checking for data distribution normality (Shapiro-Wilk). *Post-hoc* multiple pairwise comparison tests (Dunn's and Wilcoxon's signed-rank tests using Benjamini-Hochberg correction) were also performed when significant differences were observed ($p < 0.05$). A principal component analysis (PCA) was performed to test the relationships between monitored physiological parameters in order to assess the overall thermal acclimation response of both *Ostreopsis* species. All statistical analyses were conducted using R v4.3.1 software (R Core Team, 2023).

The use of a modelling approach allowed for making a smoothened representation of growth rate variations as a function of temperature. More interestingly, it also generated estimations of the minimal and maximal temperatures defining the thermal niche, as well as the optimal temperature for growth. Those values could thus be different from the levels of temperature tested during the experiment, in the intervals or out of the range. The dataset was fitted to several growth models: four of them are described by Tian (2006) and so called the "Thebault", "Beta", "exponential product" and the "modified exponential" non-linear functions, the last one was defined by Bernard and Rémond (2012). Non-linear regressions and estimation of modelling parameters were performed using Statgraphics Centurion 18®. Among those models, the non-linear "exponential product" function (Kamykowski and McCollum, 1986) generated the best fit ($r^2 = 0.81$ for *O.* cf. *siamensis*; $r^2 = 0.75$ for *O.* cf. *ovata*) compared to others ($r^2 \leq 0.58$). This function is described by the following equation:

$$\mu(T) = \left(1 - e^{-\alpha(T - T_{min})}\right)\left(1 - e^{-\beta(T_{max} - T)}\right)$$

Where μ is the growth rate at a T given temperature (°C), T_{min} and T_{max} are the lowest and highest temperatures under which the corresponding biological rate is zero, and α and β are constants.

For toxicity analysis, mortality rates of *A. franciscana* were used to calculate LC_{50} and LC_{30} after 24 and 48 h of exposure, which correspond to the cell concentrations of *Ostreopsis* cells causing 50 % and 30 % of nauplii mortality. LT_{50} and LT_{30} at 400 cells.mL^{-1}, which correspond to the time needed for *Ostreopsis* cells to cause 50 % and 30 % of nauplii mortality, was also calculated. These values were estimated following probit regression models using a sigmoidal log-response curve from the R package "ecotox".

3. Results

3.1. Growth abilities

3.1.1. Strains screening at 22 °C

Under the temperature of 22 °C, the 17 strains of *O.* cf. *siamensis* and the 3 strains of *O.* cf. *ovata* were characterized by mean growth rates in exponential phase that ranged from 0.44 d^{-1} ± 0.10 d^{-1} (*O.* cf. *ovata* strain MCCV99) to 1.25 d^{-1} ± 0.22 d^{-1} (*O.* cf. *siamensis* strain Z6) (Figure 2, Supplementary Table 2). Out of these 20 strains, 6 showed values of μ_{max} higher than 0.9 d^{-1} and were all belonging to the species *O.* cf. *siamensis*. These strains were isolated from either Zierbena, San Sebastian or Hondarribia, three Spanish sites of the Atlantic coast. For these sites in particular, a strong variability between strains was noted in terms of growth abilities, with, for example, values of strain-specific μ_{max} ranging from 0.67 to 1.25 d^{-1} for the site of Zierbena or from 0.75 to 1.19 d^{-1} for San Sebastian. Pooling all strain-specific μ_{max} data at 22 °C together, an overall significant difference between the sites was observed in terms of growth abilities (Kruskal-Wallis, $p < 0.05$). No significant difference between sites for *O.* cf. *siamensis* could be identified, however; the only significant difference was related to higher μ_{max} obtained for *O.* cf. *siamensis* strains from Zierbena (Atlantic coast, Spain) compared to *O.* cf. *ovata* strains from Rochambeau (Mediterranean Sea, France) (post-hoc Dunn's test, $p < 0.05$; Figure 2).

3.1.2. Acclimation to temperature gradient

Over the acclimation experiment, the nine strains of *O.* cf. *siamensis* tested were all able to grow and acclimate at temperatures ranging from 16 °C to 25 °C (Figure 3A, Supplementary Table 2). Out of this range, most of the strains showed a drastic response to the last change in temperature (From 25 °C to 28 °C or from 16 °C to 14.5 °C), characterized by a sudden stop of swimming activity and cell division that ended in cell death after few

weeks; still, one strain of each site (Z1, H10 and SJL1) was able to acclimate to 14.5 °C and be maintained at this temperature with a low but stable μ_{max} that ranged between 0.04 d^{-1} and 0.13 d^{-1} (Figure 3A). Under 28 °C, only two strains (Z7 and Z8) were able to grow over few weeks, but could not reach thermal acclimation.

For *O.* cf. *ovata*, the range of temperature over which cells were able to grow and be maintained was larger and defined by higher minimal and maximal values of temperature than for *O.* cf. *siamensis*. The three strains from the Mediterranean Sea were acclimated to temperatures ranging from 19 °C to 30 °C and the MCCV98 strain was even successfully maintained at 32 °C with a high μ_{max} of 0.42 d^{-1} ± 0.01 d^{-1} (Figure 3B, Supplementary Table 2). A decrease in temperature from 19 °C to 16 °C stopped cell division of all *O.* cf. *ovata* strains and induced a death of all cultures over few weeks.

Within the thermal niche of *O.* cf. *siamensis*, maximal values of μ_{max} were observed at 22 °C for each of the nine strains tested during the acclimation experiment (Figure 3A). These values corresponded to an average of 0.73 d^{-1} ± 0.19 d^{-1}. For each isolation site, a significant overall difference in μ_{max} of *O.* cf. *siamensis* as a function of temperature was observed (Friedman's ANOVA, $p < 0.05$), but the post-hoc test failed to identify which temperatures were associated with it (Wilcoxon signed-rank, $p > 0.05$). When comparing μ_{max} data between sites (Zierbena, Hondarribia or Saint-Jean-de-Luz) for each temperature, no significant difference was obtained (Friedman's ANOVA, $p > 0.05$). Thus, data from the nine strains of *O.* cf. *siamensis* were then pooled together in order to characterize the relationship between growth capacities and temperature at the species level in the SE Bay of Biscay. With this larger set of data ($n = 9$), an overall significant difference was found in *O.* cf. *siamensis* growth rates as a function of temperature (Friedman's ANOVA, $p < 0.001$) and significant differences in μ_{max} were identified between every step of temperature, from 14.5 °C to 25 °C (post-hoc Wilcoxon signed-rank test, $p < 0.01$), except between 19 °C and 25 °C and between 14.5 °C and 28 °C (Figure 3A).

Similarly, for the three strains of *O.* cf. *ovata* from Rochambeau, an overall significant difference in the mean maximal growth rates was obtained as a function of temperature (Friedman's ANOVA, $p < 0.05$), but the post-hoc multiple comparison test failed to identify which temperatures were associated with it (post-hoc Wilcoxon signed-rank test, $p > 0.05$). For this other species, maximal values of μ_{max} were observed at 28 °C for the three strains tested, reaching 0.63 d^{-1} ± 0.10 d^{-1} (Figure 3B).

3.1.3. Thermal niche modelling

The convergence of a non-linear exponential product function fitted the data sets with $r^2 \geq 0.75$ for both species (Figure 3). This model simulates an increase and subsequent decrease in growth rate as a function of temperature between two threshold values, the minimal (T_{min}) and maximal (T_{max}) temperatures under which growth stops ($\mu = 0$). Pooling results from the nine strains of *O.* cf. *siamensis*, the convergence of the model was optimal for the following values of parameters: T_{min} = 14.3 °C, T_{max} = 28.0 °C, α = 0.158 and β = 0.298 (Figure 3A). The optimal temperature associated with the highest growth rate was estimated at 22.2 °C by the model. For *O.* cf. *ovata*, the optimal convergence of the model generated higher temperature thresholds than those obtained for *O.* cf. *siamensis*: T_{min} = 16.0 °C, T_{max} = 32.6 °C, the optimal temperature associated with the highest growth rate was estimated at 26.6 °C and the two constants were α = 0.094 and β = 0.325 (Figure 3B).

Maximal abundances reached in cultures followed a similar pattern than maximal growth rate as a function of temperature, more clearly defined for *O.* cf. *siamensis* than for *O.* cf. *ovata* (not shown). For *O.* cf. *siamensis* strains, highest cell concentrations at the stationary phase were obtained at 22 °C (always exceeding 10,000 cells·mL^{-1}), high levels of maximal abundance were observed at 19 °C and 25 °C (always exceeding 5,000 cells·mL^{-1}), intermediate values were recorded at 16 °C (comprised between 1,600 and 7,500 cells·mL^{-1}) and cell concentrations never exceeded 1,000 cells·mL^{-1} at 14.5 °C. For *O.* cf. *ovata* strains, levels of abundances reached at the end of the stationary phase were more variable between strains and cultures than for *O.* cf. *siamensis*. An overall relationship between variations in μ_{max} and maximal abundances was still apparent: the highest concentrations were observed at 25 °C and 28 °C (higher than 3,800 cells·mL^{-1} and sometimes exceeding 10,000 cells·mL^{-1}), slightly lower values were recorded at 22 °C (comprised between 2,000 and 9,000 cells·mL^{-1}) and even lower concentrations were reached at 19 °C, 30 °C and 32 °C (never exceeding 5,000 cells·mL^{-1}).

3.2. Toxin content and toxicity bioassays

The analyses conducted by LC-MS/MS on the 17 strains of *O.* cf. *siamensis* grown at 22 °C did not identify the presence of any PLTX-like toxin associated with the *Ostreopsis* genus (ovatoxins a-g, ostreocins a-e, ostreol-a and mascarenotoxins a-c). Contrastingly, the bioassays on *A. franciscana* nauplii did reveal a significant toxicity for every strain of *O.* cf. *siamensis*, as well as for all *O.* cf. *ovata* strains. At 22 °C, this toxicity was high: calculations of LC_{50} were lower than 50 cells·mL^{-1} over 48h of exposure for all the 20 *Ostreopsis* strains

tested except one, *O.* cf. *siamensis* strain SJL1 (Supplementary Table 3). Measurements obtained for the strain *O.* cf. *siamensis* SJL1 were associated with an uncommon mortality diagram where a higher mortality was measured at 40 cell·mL^{-1} than at 400 cell·mL^{-1} (Supplementary Figure 1). This particular characteristic was noted for most of the diagrams of mortality rates expressed as a function of *Ostreopsis* concentrations obtained for this strain, all along the temperature gradient; it induced a poor convergence of the regression model and a probable underestimation of LC_{50}. Such surprising profiles were rare and not due to excessive mortality in some control wells. Taking the acclimation experiment as a whole, only few dead *A. franciscana* nauplii were observed under control conditions over 48h of incubation and corresponded to a single or to two nauplii per control condition.

Under 14.5 °C, 16 °C and 19 °C, the threshold of 50 % of mortality was not reached after 48h of exposure at the highest cell concentration for almost half of the *O.* cf. *siamensis* strains. For these particular cases, a poor precision of LC_{50} estimations can be suspected. To avoid such doubt, the parameters LC_{30} and LT_{30} were used instead of LC_{50} and LT_{50} to assess the differences in toxicity among strains and graded temperature conditions (Figure 4).

For *O.* cf. *siamensis*, when comparing toxicity levels between sites (H, Z or SJL, with three strains per site), no significant difference in LC_{30} or LT_{30} values were observed (Friedman's ANOVA, $p > 0.05$) at any of the temperatures tested. Thus, a subsequent analysis was performed pooling data from the nine strains of *O.* cf. *siamensis* together, in a way to characterize the toxic risk at the species level in the SE Bay of Biscay. A significant decrease in toxicity with decreasing temperature was observed between 16 °C and 22 °C and this trend was coherent with values obtained for the only strain (Z8) monitored at 14.5 °C. It was both noted from variations of LC_{30} (Friedman's ANOVA, $p < 0.01$; Wilcoxon signed-rank test, $p < 0.05$; Figure 4A) and LT_{30} (Friedman's ANOVA, $p < 0.01$; Wilcoxon signed-rank test, $p < 0.05$; Figure 4B).

Concerning *O.* cf. *ovata*, no overall significant difference was observed in terms of toxicity on *A. franciscana* between the temperatures ranging from 19 °C to 30 °C for both LC_{30} (Figure 5C) and LT_{30} (Figure 5D) values. However, a trend similar to the one observed for the toxic response of *O.* cf. *siamensis* to varying temperature conditions was observed on the LT_{30} parameter: LT_{30} values of *O.* cf. *ovata* strains regularly increased with decreasing temperature from 28 °C to 19 °C (Figure 5D), *i.e.* for temperatures equal and below the optimal temperature tested for growth. The lack of statistical significance of these variations was probably due to the low number of strains used for this species ($n = 3$). Values obtained for the only strain measured at 32 °C (MCCV98) were coherent with this trend.

3.3. Indicators of stress and acclimation

3.3.1. Pigment composition

The two *Ostreopsis* species showed similar pigment profiles (Table 1). Chlorophyll related pigments were dominated by chlorophyll *a* (Chl *a*) and chlorophyll c_2. Carotenoids included peridinin, β-carotene and the xanthophyll cycle pigments Dd and Dt. Amongst other xanthophyll pigments of interest for dinoflagellates, dinoxanthin was not detected, while violaxanthin and zeaxanthin were only detected at very low concentrations and not in every sample.

Throughout the thermal acclimation gradient, the β-carotene:chlorophyll ratio remained stable for both species, with average values of 0.032 (±0.005) for *O.* cf. *siamensis* and 0.027 (±0.006) for *O.* cf. *ovata*. In *O.* cf. *siamensis*, the total amount of pigments of the diadinoxanthin cycle, (Dd+Dt)/Chl *a*, increased with decreasing temperature (Fig. 5A). This trend was significant from 25 °C to 16 °C (Friedman's ANOVA, $p < 0.01$). Among them, Dd/Chl *a* ratio showed a similar and significant trend from 25 °C to 19 °C (Wilcoxon's signed-rank tests, $p < 0.05$), then a stabilization between 19 °C and 16 °C and a decrease towards 14.5 °C. Variations of Dt/Chl *a* were different: this ratio remains stable between 25 °C and 19 °C, then significantly increased at 16 °C (Friedman's ANOVA, $p < 0.01$; Wilcoxon's signed-rank tests, $p < 0.05$). The DES was also shown to be significantly higher at 16 °C than at higher temperatures (Friedman's ANOVA, $p < 0.01$; Wilcoxon's signed-rank tests, $p < 0.05$) (Fig.5C). Measurements obtained for two strains at 14.5 °C corroborated this trend: Dt became the major pigment present for the diadinoxanthin cycle at this temperature with DES reaching 0.62.

In *O.* cf. *ovata* however, no significant changes in xanthophyll cycle ratios were observed (Friedman's ANOVAs, $p > 0.05$) across the temperature gradient (Fig. 5B and 5D).

3.3.2. Lipid composition

The composition of lipids in *Ostreopsis* species was assessed throughout the thermal acclimation gradient by measuring the cellular quotas of different lipid classes, including neutral lipids, phospholipids and glycolipids. Total lipid concentrations ranges were relatively similar between *O.* cf. *ovata* (0.65 – 2.64 ng·cell^{-1}) and *O.* cf. *siamensis* (0.61 – 3.04 ng·cell^{-1}). In addition, ranges of proportions of the different lipid classes were similar between the two species, with neutral lipids representing the most abundant class (50.5 – 62.5 % for *O.* cf.

ovata and 40.7 – 54.1 % for *O.* cf. *siamensis*), followed by phospholipids (26.7 – 31.3 % for *O.* cf. *ovata* and 30.2 – 42.4 % for *O.* cf. *siamensis*) and then by glycolipids (10.8 – 18.2 % for *O.* cf. *ovata* and 16.8 – 21.1 % for *O.* cf. *siamensis*).

For *O.* cf. *siamensis*, the total amount of lipids per cell reached a minimum at 22 °C. A significant increase with decreasing temperature was also observed between 16 °C and 22 °C (Friedman's ANOVA, $p < 0.01$; Wilcoxon's signed-rank test, $p < 0.05$; Fig. 6A). This trend was apparent for every lipid classes, but only significant for glycolipids and phospholipids (Friedman's ANOVAs, $p < 0.05$, Wilcoxon's signed-rank tests, $p < 0.05$). Measurements obtained for Z8 at 14.5 °C were in agreement with these trends, either for each lipid class or for the total lipid content (Fig. 6A). Throughout the acclimation gradient, variations of the proportion of each lipid class were weak, if any. No significant variation in proportions of neutral lipids and phospholipids was observed with temperature over the range 16 °C - 25 °C (Fig. 6C). For glycolipid proportions, significant differences as a function of temperature were observed (Friedman's ANOVA, $p < 0.05$) but the post-hoc pairwise comparison test failed to identify how.

Concerning *O.* cf. *ovata*, total lipid concentrations exhibited lowest values under intermediate temperatures (22 °C and 25 °C) and a maximum under the coldest temperature tested (19 °C) that was about four times higher (Fig. 6B). These variations in relation to temperature were similar in every lipid classes, but were not significant in most of the cases, probably because of the small amount of samples (n=3) (Fig. 6B). Overall, significant differences were observed in neutral lipid and phospholipid concentrations (Friedman's ANOVA, $p < 0.05$), but the post-hoc test failed to determine which temperatures differed from one another. Variations in cellular contents of total lipids and glycolipids with temperature were not significant. When considering proportions, significant differences related to temperature were only observed for neutral lipids and phospholipids (Friedman's ANOVAs, $p < 0.05$). They were not associated with any visible trend and the post-hoc test failed to determine which temperatures were leading them (Fig. 6D).

3.3.3. Cell distribution in cultures

A difference in cell repartition was noted for *O.* cf. *siamensis* cultures maintained under the cold temperatures of 16 °C and 14.5 °C. For cultures growing at 19 °C, 22 °C and 25 °C, cells were mostly accumulated either on the bottom of the flask during the exponential phase and decline phase, or in mucilaginous aggregates floating in the medium at the end of the

exponential phase. They were also strongly aggregating when cultures were gently mixed, prior to samples' collection, making the homogenization of cultures complex for sub-sampling. Such characteristics and behaviour were not observed under cold temperatures: at 16 °C and 14.5 °C, *O.* cf. *siamensis* cells were mainly spread in the whole volume of medium and cultures were easy to homogenize as no strong aggregates of cells were created after gentle mixing.

3.4. Merged acclimation response to temperature and relationship between parameters

A multivariate analysis (PCA) was performed for each *Ostreopsis* species on data measured from 12 strains throughout the thermal acclimation gradient. It compiled indicators related to growth (μ_{max}), toxicity (LC 30 and LT 30), xanthophyll-related pigments (DES and (Dd+Dt)/Chl *a* ratios) and lipid composition (concentrations of neutral lipids, glycolipids and phospholipids), as well as temperature which was added as an illustrative variable. Only data obtained for temperatures ranging from 16 °C to 25 °C for *O.* cf. *siamensis* and from 19 °C to 30 °C for *O.* cf. *ovata* were retained for the PCA analysis. Indeed, every parameter was estimated for all the strains of each species under these temperatures, but not for the two extremes 14.5 °C and 32 °C.

The first two principal components of *O.* cf. *siamensis* PCA score plot explained more than 74% of the total inertia of projected variables (Fig. 7A), indicating a good representation of the relationship between parameters (Supplementary figure 4). The most important variables contributing to the first factorial axis of the PCA (54.5 % of the total inertia) were the concentrations of each lipid class (0.85 to 0.91), indicators of toxicity (0.82 and 0.63) and μ_{max} (-0.62) (Supplementary figure 4). The second axis was driven by the (Dd+Dt)/Chl *a* ratio (-0.81), the concentration of neutral lipids (0.45), DES (-0.43) and μ_{max} (0.40) and captured 20.3% of the variation. These results indicate that the first factorial axis of the PCA discriminates strains responses to temperature according to their concentrations in lipids, their toxicity level and their growth ability, while the second factorial axis highlights the role of the xanthophyll pigments. Strains with relatively high growth rate exhibited low content in lipids, high toxicity and a low level of activation of the xanthophyll cycle (low (Dd+Dt)/Chl *a* ratio and low DES). The temperature variable was strongly positively correlated to the first axis (r^2=0.62) and mildly positively correlated to the second (r^2=0.24). In the end, clusters of

individuals grouped by temperature separated from each other diagonally (Fig. 7A), showing different overall physiological states of the strains in response to temperatures.

Regarding *O.* cf. *ovata*, the factorial space of the PCA formed by the first two axes explained more than 75% of the total inertia of projected variables (Fig. 7B), once again indicating a good representation of the relationship between parameters (Supplementary figure 4). The most important variables for the construction of the first factorial axis of the PCA (51.2 % of the total inertia) were the concentrations of neutral lipids (0.90) and phospholipids (0.80), the (Dd+Dt)/Chl *a* ratio (0.89), LC30 (0.85) and μ_{max} (-0.60). The second axis was driven by the concentrations of glycolipids (0.82) and phospholipids (0.58), the level of LT30 (-0.61) and also μ_{max} (0.54) and captured 24.5% of the inertia. Similarly to *O.* cf. *siamensis*, strains exhibiting high growth rates showed a high toxicity and a low level of xanthophyll pigment content. However, the relationship between growth rate and the content of lipid classes was not as clear as for the other species. Temperature was strongly correlated to both first (r^2=0.74) and second (r^2=0.84) axis. In the end, clusters of individuals grouped by temperature were strongly separated, indicating different physiological states of the strains activated all along the temperature gradient tested (Fig. 7B).

4. Discussion

4.1. Optimal growth according to temperature for *O.* cf. *siamensis* and *O.* cf. *ovata*

The characterization of optimal growth temperature is crucial for the investigation of species ecology, especially in a context of global warming where marine microalgae communities and productivity will be affected by rising temperatures (Behrenfeld *et al.*, 2006; Morán *et al.*, 2010; Sepúlveda and Cantarero, 2022). A thermal acclimation experiment was conducted on both species *O.* cf. *siamensis* and *O.* cf. *ovata* testing a large temperature gradient (from 14.5 °C to 32 °C) with short temperature intervals (1.5 °C to 3 °C). The temperature of 22 °C was identified as the optimal one for the growth of the nine *O.* cf. *siamensis* strains tested (all isolated from the Bay of Biscay), both in terms of growth rate (from measurements and modelling approach) and cell density. Using three strains of *O.* cf. *ovata* (all isolated from Villefranche-sur-Mer, NW Mediterranean Sea), the optimal temperature for growth of this other species was estimated at 27 °C and 28 °C from modelling approach and measurements, respectively. These values are in accordance with previous works, where maximum growth rates of *Ostreopsis* cells in cultures were reported at temperatures ranging from 20 °C to 30

°C for *Ostreopsis* cf. *ovata* (Pezzolesi *et al.*, 2012; Tawong *et al.*, 2015; Carnicer *et al.*, 2016; Yamaguchi *et al.*, 2012; Gémin *et al.*, 2021) and *Ostreopsis* sp.1, sp.6 and sp.7 (Tanimoto *et al.*, 2013; Tawong *et al.*, 2015).

Growth abilities of 17 strains of *O.* cf. *siamensis* were characterized at 22 °C and showed a strong variability between strains, with μ_{max} varying between 0.54 and 1.25 d^{-1}. For the Spanish sites of Zierbena, Hondarribia and San Sebastian in particular, six strains showed μ_{max} superior to 0.9 d^{-1}, corresponding to high values compared to rates usually reported for dinoflagellates. Dinoflagellate growth rates are mostly lower than 1.0 d^{-1}, when diatoms and various flagellate taxa are known to often exceed this threshold value (Smayda, 1997; Sarthou *et al.*, 2005; Litchman *et al.*, 2007). Low growth ability is even reported as one of the main functional traits of dinoflagellates, partly explained by poor abilities of cells to take up nutrient sources (Litchman *et al.*, 2007). Despite this general assumption, extremely high growth rates (> 1 d^{-1}) were reported for some dinoflagellate species (Smayda, 1997), and more precisely for some clones of dinoflagellates. For instance, optimal growth rates of several clones of *Alexandrium catenella* and *Alexandrium tamarense* ranged from 0.28 to 1.0 d^{-1} and from 0.23 to 1.03 d^{-1}, respectively (Smayda, 1997; Laabir *et al.*, 2011). This shows that competitive abilities can be highly strain-specific. In the present study, the strains of *O.* cf. *siamensis* that grew at μ_{max} close to or higher than 1.0 d^{-1} showed growth abilities equivalent to fast growing phytoplankton groups, such as diatoms, coccolithophorids or green algae (Litchman *et al.*, 2007). Thus, it can be expected that the observed strain diversity promotes a successful colonization and extension of the habitat of *O.* cf. *siamensis* populations in the Bay of Biscay.

Such high maximal growth rate strategy cannot be defined for *O.* cf. *ovata*, at least not in coastal waters of the Mediterranean Sea. In the present study, estimations of maximal growth rates for *O.* cf. *ovata* strains reached maximum values between 0.52 and 0.70 d^{-1}. Such characteristics of growth abilities are in accordance with previous laboratory studies done for other Mediterranean strains of *O.* cf. *ovata*: reported μ_{max} values range from 0.32 d^{-1} to 0.83 d^{-1} (Guerrini *et al.*, 2010; Pezzolesi *et al.*, 2012; Scalco *et al.*, 2012; Ben-Gharbia *et al.*, 2016; Jauzein *et al.*, 2017; Gémin *et al.*, 2021; Medina-Pérez *et al.*, 2023). Only one strain of *O.* cf. *ovata* from Japan was characterized by a μ_{max} higher than 1 d^{-1}, reaching 1.03 d^{-1} between 25 °C and 30 °C (Yamaguchi *et al.*, 2012). For this species, part of its ecological success may not rely on investing more energy to maximize its growth rate, but on allocating more resources to maximize its competitive ability and survival (e.g. through the production of

secondary metabolites or mucilage). Additionally, its success would rely on the size of its environmental niche, in particular the thermal one.

4.2. Acclimation strategy towards temperature

Any change of temperature induces a cellular response in microalgal cells, associated with a disruption of homeostasis and activation of stress pathways (Borowitzka, 2018). In response, cells can modify their metabolism and regulate physiological functioning during an acclimation process in order to restore homeostasis. If a new state of equilibrium can be reached, cells are able to grow under the new environmental conditions; if not, cells die, potentially after the formation of quiescent stages, such as temporary cysts in *Ostreopsis* cells (Bravo *et al.*, 2012).

For the nine strains of *O.* cf. *siamensis* and the three strains of *O.* cf. *ovata* tested, moving away from the optimal temperature of 22 °C and 28 °C, respectively, induced a net decrease in growth rate associated with acclimation to non-optimal growth conditions. Different pathways were studied in order to define physiological modifications allowing for such acclimation to temperature.

The lipid quantity and composition of cells can reflect ability of marine microorganisms to adapt to environmental changes (Thompson, 1996; Guschina and Harwood, 2009). In our study and for both *Ostreopsis* species, the total amount of lipids per cell was minimal under optimal growth temperatures. Similar trends of total lipid content in microalgae were reported as a function of temperature, but also of other stressful environmental conditions such as nutrient depletion or light intensity (Sharma *et al.*, 2012; Sun *et al.*, 2018). Interestingly, in *Ostreopsis* cells, these variations were apparent for every lipid class, allowing for pointing out some specific aspects of their thermal acclimation processes.

For neutral reserve lipids (apolar), the highest concentrations in *Ostreopsis* cells were obtained under extreme temperatures. This trend was apparent on both edges (cold and warm) of the thermal niche of *O.* cf. *ovata*, but only visible under extremely low temperatures for *O.* cf. *siamensis*. This is in accordance with results observed in various microalgae species where neutral lipids were accumulated under unfavourable conditions (Sharma *et al.*, 2012). Neutral lipids are mainly composed of fatty acids (FAs), predominantly saturated ones, which can serve as a source of carbon and energy (Sharma *et al.*, 2012). Their accumulation under stressful conditions allows for the storage of compounds able to sustain basal metabolism or

growth in case nutrition fluxes or photosynthesis become insufficient. Interestingly, only *O.* cf. *ovata* activated this storage pathway under warm temperatures as part of the acclimation process.

For polar lipids, phospholipids and glycolipids, the lowest concentrations were obtained under optimal growth temperatures, as reported for various microalgae species (Gašparović *et al.*, 2013; Novak *et al.*, 2018, 2019). If lowering temperature led to an increase in both phospholipids and glycolipids for the two *Ostreopsis* species, warm temperatures only induced it for *O.* cf. *ovata*. These polar lipids are structural components of membranes (Sharma *et al.*, 2012), with phospholipids and glycolipids considered to be the main constituents of either the cell membrane or the chloroplast, respectively (Harwood, 1998; Guschina and Harwood, 2009). Polar lipids also tend to have relatively high content of poly-unsaturated fatty acids (PUFAs) (Sharma *et al.*, 2012). This characteristic is of particular interest when considering temperature acclimation processes. Indeed, a known effect of temperature on cell membranes refers to their flexibility. Cold temperatures are known to reduce it in photosynthetic organisms (Somerville and Browse, 1996). In response, cells can increase their level of PUFAs: these compounds have a high number of double bonds, so they can help restoring the cell membrane fluidity. Even if cell size was not measured in the present study, this process can partly explain the increase in polar lipid contents of *Ostreopsis* cells in response to cold temperatures. On the other hand, an increase in saturated FAs over the formation of PUFAs was also expected for controlling membrane rigidity under high temperatures (Renaud *et al.*, 1995; Murata and Los, 1997; Sharma *et al.*, 2012). Estimations of phospholipids' content of *O.* cf. *siamensis* seem to fit to this concept as they did not seem to vary between optimal and warm temperatures. Conversely, for *O.* cf. *ovata* cells, high cellular content of phospholipids and glycolipids were measured under warm temperatures. A more detailed characterization of these lipids, including their saturation level, and measurements of cell size are required to explain such trend. Estimations of specific glycolipids such as monogalactosyldiacylglycerol (MGDG) and digalactosyldiacylglycerol (DGDG) will be of particular interest because they are known to be implied in thermotolerance of dinoflagellate cells (Sakurai *et al.*, 2007; Mizusawa *et al.*, 2009). MGDG and DGDG form the structural matrix containing proteins and photosynthetic pigments involved in photosynthesis (Jones, 2007; Kern *et al.*, 2009) where they can have a role in the management of oxidative stress.

In marine organisms, a common sign of transient response to thermal stress is the over-production of reactive oxygen species (ROS) in the cells. It is linked to both the role of

ROS as signalling molecules in stress pathways and/or to the disruption of production sites of ROS (Lesser, 2006; Jauzein and Erdner, 2013). An excess of intracellular ROS can be deleterious to cells by damaging macromolecules and even activating death pathways (Triantaphylidès and Havaux, 2009). Marine microalgae have several ways to control such oxidative stress (Lesser, 2006) in order to support acclimation. The pigment composition is one of them. Indeed, it can play on both ROS production sites (photosynthetic pigments) and ROS scavenging capacities (carotenoids and xanthophyll cycles) (Cirulis *et al.*, 2013; Goss and Lepetit, 2015). For instance, some carotenoids, including β-carotene, are known for their antioxidant properties (Cirulis *et al.*, 2013; Zuluaga *et al.*, 2017). In addition, xanthophyll cycles (XCs) play a major role in the non-photochemical quenching (NPQ), a photoprotective mechanism preventing damages cause by oxidative stress on the photosynthesis machinery (Goss and Jakob, 2010; Latowski *et al.*, 2011; Kuczynska *et al.*, 2015). Lipid-associated XC pigments can also directly act as ROS scavengers (Kuczynska *et al.*, 2015). In marine microalgae, the two main XCs are based on the interconversion of the pigment couple Dd/Dt or the trio violaxanthin (V)/ antheraxanthin (A)/ zeaxanthin (Z) (Kuczynska *et al.*, 2015). According to the pigment profiles found in the present study, all *Ostreopsis* strains showed combinations corresponding to the type I chloroplast reported by Zapata *et al.* (2012): the peridinin-type characteristic of dinoflagellate species. In such pigment composition, ROS accumulation can be managed by both a modification of the β-carotene:chlorophyll ratio and an activation of the XC cycle Dd/Dt. In *Ostreopsis* spp. strains tested, the β-carotene:chlorophyll ratio stayed stable all over the temperature gradient, but an activation of the XC cycle Dd/Dt was observed. Interestingly, this activation was species-specific: it was only apparent for *O.* cf. *siamensis*, not for *O.* cf. *ovata*. No other XC cycle was identified in *Ostreopsis* cells as V and Z were only occasionally present, without any proof of conversion of V into Z, and no Dn was detected.

In microalgae, variations in content and composition of carotenoids can be part of the acclimation process to adverse conditions (Demmig-Adams and Adams, 2006; Demmig-Adams *et al.*, 2014), such as changes in irradiance (Dubinsky and Stambler, 2009) or temperature (Thompson *et al.*, 1992a, 1992b; Kana *et al.*, 1997). Interestingly, studies suggested that photochemical acclimation to low temperatures mimics acclimation to high irradiance (Davison, 1991; Mock and Hoch, 2005). In *O.* cf. *siamensis*, activation of the Dd/Dt cycle was noted from concomitant variations of DES (hallmark of the conversion between Dd and Dt) and (Dd+Dt)/Chl *a* (indicator of the total quantity of XC pigments): both parameters increased with decreasing temperature. Similarly, low temperatures were

associated with an increase in both (Dd+Dt)/Chl *a* and Dt/Chl *a* ratios in diatoms (Anning *et al.*, 2001; Lacour *et al.*, 2018, 2022). Such acclimation process can be a response to decreased carbon-fixation capacity of phytoplankton at low temperatures (Young *et al.*, 2015): the slowing down of growth can create an unbalance between fluxes of energy and C assimilation. In this case, the excessive absorbed light energy has to be dissipated by the cell as heat, using XCs and NPQ mechanisms, in order to maintain photostasis (Fanesi *et al.*, 2016). Under warm temperatures, some studies reported similar acclimation processes based on XCs (Salleh and McMinn, 2011; López-Rosales *et al.*, 2014; Laviale *et al.*, 2015). This was not the case in our study: for both *Ostreopsis* species, other pathways than pigment composition modulation support acclimation to high temperatures.

In the present study, abilities to rely on XC for managing stressful conditions were identified for all *O.* cf. *siamensis* strains but not for *O.* cf. *ovata*. Interestingly, NPQ and XC characteristics were shown to vary amongst species (Lavaud *et al.*, 2007; Giovagnetti *et al.*, 2012; Quaas *et al.*, 2015), but also amongst ecotypes (Six *et al.*, 2009; Bailleul *et al.*, 2010; Stamenković *et al.*, 2014), meaning that they can be the result of ecological niche adaptation (Petrou *et al.*, 2011; Lavaud and Goss, 2014). For instance, Lacour *et al.* (2020) observed that upon a variety of microalgae groups, species developing in high light fluctuations ecosystems, such as tidal zones, exhibited higher NPQ efficiencies than species developing in lower light fluctuations habitats. Similarly, retention of Z and Dt (de-epoxidation stages of XCs) have been reported in microalgae acclimated to high variations of light and temperature (Perkins *et al.*, 2010; Berne *et al.*, 2018; Lacour *et al.*, 2018). In our study, strains of *O.* cf. *siamensis* were isolated from tidal ecosystems, where daily light and temperature variations are high, whereas *O.* cf. *ovata* strains were isolated from sheltered areas exhibiting low environmental variations. Thus, the cause of differences in XC activation between *Ostreopsis* strains should still be considered as an open question: is it a mark of a difference in acclimation strategy between species or the result of long-term acclimation to drastically different habitats? The answer needs further analyses focusing on ecotypes of the two species, comparing strains isolated in the Bay of Biscay (tidal environment) to strains isolated in the Mediterranean Sea.

When considering roles of lipids and pigments in species-specific acclimation strategy, their interconnection is also crucial. Indeed, XCs are strongly dependent on the lipid composition of thylakoid membranes (Goss and Latowski, 2020). In particular, the solubilisation of the Dd de-epoxydase enzyme, responsible for the conversion of Dd into Dt, requires the presence of the glycolipid MGDG (Latowski *et al.*, 2004; Goss *et al.*, 2005, 2007; Lepetit *et al.*, 2012). In the present study, the increase in XC pigments per cell and in DES for

O. cf. *siamensis* was observed as soon as temperature became lower than the optimum and was concomitant with a net increase in glycolipids' content. A similar but not significant trend was noted for *O.* cf. *ovata*. Thus, a more detailed characterization of lipids as a function of temperature is required in order to define if lipid composition could be the limiting factor for the activation of XC in strains of *O.* cf. *ovata* in response to cold temperatures. Estimations of the MGDG pool in the thylakoid membrane would be of great interest in order to go this step further.

In the end, species-specific acclimation processes described in the present study led to differences in thermal niches. In accordance with what can be expected from the activation of XC, *O.* cf. *siamensis* showed better abilities to grow under cold temperatures than *O.* cf. *ovata*. This species was also characterized by a less extensive thermal niche (from 14.5 °C to 25 °C, covering a 10.5 °C range) than *O.* cf. *ovata* (at least from 19 °C to 32 °C, covering a 13 °C range). Unfortunately, it is not possible to clearly state a reason why the thermal niche of *O.* cf. *ovata* creates more growth opportunities than the one of *O.* cf. *siamensis* yet, in particular at warm temperatures. Part of the answer might rely on the lipid composition of the cells, especially regarding the presence of MGDG in membranes.

4.3. Toxicity and temperature

A large number of studies conducted on *Ostreopsis* toxicity focused on the characterization of toxins produced by *O.* cf. *ovata* strains, especially isobaric palytoxin and ovatoxins (Ciminiello *et al.*, 2012, 2011, 2010). Strains of *O.* cf. *ovata* from the Mediterranean Sea, including the ones used in the present study, are able to produce a high diversity of palytoxin analogs such as ovatoxins (Pavaux *et al.*, 2020a). They are also known for impacting other members of the marine plankton community such as grazers and other microalgae (Ternon *et al.*, 2018; Pavaux *et al.*, 2019, 2020a, 2020b). For *O.* cf. *siamensis*, little is known about the potential production of toxic or allelopathic compounds, except that no PLTX-like compounds were found so far. In the present study, as well as in Laza-Martinez *et al.* (2011), strains of *O.* cf. *siamensis* from the Bay of Biscay exhibited toxic effects on *Artemia franciscana* nauplii. These effects are not due to already known toxins: the LC-MS/MS analyses could not detect any PLTX-like described so far. Similarly, both Ciminiello *et al.* (2013) and Chomérat *et al.* (2022) did not observe the presence of either ovatoxins or ostreocins in Atlantic and Mediterranean strains of *O.* cf. *siamensis*. Only traces of isobaric palytoxin were detected (< 1 $fg \cdot cell^{-1}$), and no peak could be associated with previously

characterized palytoxin-like compounds (Ciminiello *et al.*, 2011). After observing no death in a mouse bioassay, they concluded in a total absence of toxicity in both Atlantic and Mediterranean strains *O.* cf. *siamensis*. The compounds responsible for effects of *O.* cf. *siamensis* reported on *A. franciscana* are still currently unknown.

Toxicity bioassays using *Artemia* spp. are cheap, sensitive and allow for comparing toxicity among diverse organisms (Vanhaecke *et al.*, 1981; Pavaux *et al.*, 2020b). In the present study, despite the lack of any known toxin for *O.* cf. *siamensis*, maximal values of cellular toxicity were high and similar between the two species. All *O.* cf. *siamensis* strains except one (SJL1, the one showing unusual mortality diagrams) exhibited maximal toxicity from LC_{50} < 10 cells·mL^{-1} over 48h; *O.* cf. *ovata* strains had a maximal toxicity characterized by $LC_{50} \leq 3$ cells·mL^{-1} over 48h. These estimations of toxicity are in accordance with previous studies reporting bioassays on *Artemia franciscana* and *A. salina* (Pavaux *et al.*, 2020a, 2020b), where LC_{50} for *O.* cf. *ovata* ranged from 1 to 25 cells·mL^{-1}. Estimations of maximal LC_{50} obtained over the shorter time scale of 24h in the present study (30 – 400 cells·mL^{-1}) were slightly higher but coherent with values reported in the literature (< 1 – 100 cells·mL^{-1}). For *O.* cf. *ovata*, it was proven that part of this lethal effect on *Artemia* is directly due to the presence of ovatoxins and, at a lesser extent, isobaric -palytoxin (Pavaux *et al.*, 2020b). Interestingly, present results prove that unknown compounds are also contributing a lot in toxic effects of the genus *Ostreopsis*. They even account for all the high toxicity of *O.* cf. *siamensis* towards the target species *A. franciscana*.

A clear relationship between toxicity and temperature was revealed in *Ostreopsis* cells. Under temperatures colder than the optimal one, all strains of *O.* cf. *siamensis* showed a decrease in toxicity (increase in LT_{30} and LC_{30}) with decreasing temperature and a similar trend was observed for *O.* cf. *ovata* strains. Conversely, the toxic effect of *Ostresopsis* cells on *A. franciscana* did not significantly increase when temperature changed from the optimal to higher ones. Only few studies report variations of *Ostreopsis* toxicity as a function of temperature and they did not focus on *O.* cf. *siamensis*. For *O.* cf. *ovata*, some Mediterranean strains were characterized, but only across two or three levels of temperature and the associated studies sometimes depict conflicting trends. Among them, higher mortality rates of *A. franciscana* exposed to *O.* cf. *ovata* were observed at 25 °C compared to 20 °C (Faimali *et al.*, 2012; Pezzolesi *et al.*, 2012), but also to 30 °C (Pezzolesi *et al.* 2012). In Pezzolesi *et al.* (2012), the highest toxin content was also measured at the intermediate temperature of 25 °C. However, observations done with the strain MCCV54 (one of the *O.* cf *ovata* strains of the present study) by Gémin *et al.* (2021) did not show the same pattern. For MCCV54, a higher

toxin content was observed at 23 °C compared to both the optimal temperature 27 °C and a higher one (30 °C). These last results describe a trend reverse to the toxicity gradient shown in the present study. Some explanations can justify such a divergence. First, in Gémin *et al.* (2021), the influence of temperature on toxin content was mainly apparent for cells in late growth phase and plateau; values obtained in exponential phase (comparable to results of the present study) did not show that much of a difference between conditions. Second, this comparison between studies and techniques suggest that most of the lethal effect measured on *A. franciscana* should not be attributed to known toxins, or at least not directly related to the intracellular toxin pool.

For *Ostreopsis*, different hypotheses can explain an influence of temperature on toxicity: it could come from a direct influence of temperature on the synthesis or release of toxin and/or allelochemicals, to an indirect effect on growth and cell division, but also to an indirect effect on toxic compounds' repartition in the medium. This last option is supported by current results. Indeed, along with a decrease in toxicity, *Ostreopsis* cells (*O.* cf *siamensis* in particular) lost their abilities to create aggregates under extreme cold temperatures. This modification played on cells' repartition and suggests strong changes in quantity or quality of the excreted mucus. Under favourable growth conditions, the mucus surrounding *Ostreopsis* cells is known to concentrate released molecules by limiting their diffusion in the extracellular medium (Guadayol *et al.*, 2021). For toxic compounds in particular, previous studies observed that allelochemicals produced by *O.* cf. *ovata* would only affect competitors (*Licmophora paradoxa*; Ternon *et al.*, 2018) or other target organisms (*A. franciscana*; Pezzolesi *et al.*, 2012; Faimali *et al.*, 2012) in a case of a close encountering. This suggests that toxicity may rely on allelochemicals adsorbed onto the cell or localized in the "viscosphere" around *Ostreopsis* cells as defined by Guadayol *et al.* (2021). The active role of the mucus on the toxicity of *O.* cf. *ovata* was further confirmed by Giussani *et al.* (2015). In this last study, the mucilaginous matrix surrounding cells was responsible for significant lethal effects on *A. salina* and contained significant amount of toxins, when the culture medium devoid of cells and mucilage (filtered on 0.2 µm) did not. Thus, under optimal temperature conditions, the viscosity of the excreted mucus create hot spots of toxicity around *Ostreopsis* cells. Results of the present study suggest that cold temperatures reduce them because the loss of abilities to create aggregates was concomitant with a decrease in toxicity. A direct effect of temperature on mucus characteristics cannot explain these variations because cold is known to increase viscosity properties of fluids. Biological modifications of mucus are probably occurring as a function of temperature. They could be linked to changes in the production of carbohydrates

composing the mucilaginous matrix (Vidyarathna and Granéli, 2012) or a potential role of bacteria. Further studies have to be conducted in order to characterize them and define their role in toxicity along a temperature gradient, relatively to modifications of toxin production and release of allelochemicals.

4.4. Thermal niche and geographical distribution

The comparison between thermal niches estimated from laboratory experiments and field data can be highly informative, both for the study of environmental control of bloom dynamics and species geographic distribution. It can help for defining where and when temperature can be a determining factor, or a co-limiting one, for *Ostreopsis* bloom development.

In the NW Mediterranean Sea, long-term surveys of *O.* cf. *ovata* bloom phenology allowed for the estimation of a realized thermal niche for this species in South of France (Drouet *et al.*, 2022). This niche (18 °C – 28 °C) is fully in accordance with the one defined after acclimation (16 °C/19 °C – 32 °C, from model and measurements) in the present study. A strong difference between their respective limits applies to warm temperatures. It is confirmed by estimations of the optimal temperature for growth: the value obtained after acclimation (27 °C or 28 °C, from model or measurements in the present study) is much higher than the temperatures associated with maximal net growth rates in the field (21 °C - 25 °C, Drouet *et al.* (2022)). This means that, under warm temperatures in these coastal areas (>25 °C), temperature (if not optimal) is only inducing a slight limitation of cellular growth when other controlling factors, between abiotic (nutrient availability…) and biotic (grazing…) ones, are strongly limiting the populations' growth.

In the Bay of Biscay, no long-term survey of bloom dynamics of *Ostreopsis* species has been conducted so far, but a detailed spatial survey was recently carried out by Drouet *et al.* (2021). It defined limits of observation of *O.* cf. *siamensis* cells from Comillas (Spain) to Biarritz (France), a zone where sea surface temperatures (SST) are warmer than in the rest of the Bay (Costoya *et al.*, 2015). The presence of *O.* cf. *ovata* was also reported for the first time in 2021 in the same area, forming mixed assemblages with *O.* cf. *siamensis* (Chomérat *et al.*, 2022). Annual surveys of SST in this coastal zone can be compared to the species-specific thermal niches of the present study: this allows for the definition of two temporal windows during which thermal conditions are suitable for their growth. A dataset issued from the Aquarium of San Sebastian (Spain) from 2000 to 2019 revealed that temperatures between 19

°C and 25 °C were found over more than four months during the ”summer-autumn” period (Figure 8). This represents a large window, creating enough time for high developments of *Ostreopsis* populations (both *O.* cf. *siamensis* and *O.* cf. *ovata*), as long as other environmental factors are not strongly limiting their growth.

This SST monitoring in the Basque countries also revealed that the winter season is characterized by a long period (19 consecutive weeks on average) during which sea temperature drops under the 14 °C threshold defined as highly stressful for both *O.* cf. *ovata* and *O.* cf. *siamensis*. This indicates that the maintenance of *Ostreopsis* sp. populations on site has to rely on another form than growing vegetative cells to cope with winter conditions. The formation of resting cysts was identified for *O.* cf. *ovata* (Bravo *et al.*, 2012; Accoroni *et al.*, 2014). In dinoflagellates, this type of cyst is issued from sexual reproduction and can remain in a dormant stage over several months or even years (Delebecq *et al.*, 2020). To our knowledge, identification of such cysts in the cell cycle of *O.* cf. *siamensis* has not been done yet. The recurrence of *O.* cf. *siamensis* blooms in Basque countries supports their existence, but it still has to be confirmed from field surveys or crossing experiments between strains in the laboratory.

Out of the Basque countries, Drouet *et al.* (2021) found eDNA traces of *O.* cf. *siamensis* in several sites further North, reaching the western English Channel; they were interpreted as proofs of *Ostreopsis* cells' presence. The thermal niche of *O.* cf. *siamensis* estimated in the present study supports this hypothesis. Averages of weekly SST in the Bay of Brest (close to the entrance of the English Channel) were compiled over 2000-2018, from the SOMLIT (French national coastal monitoring program). They show seawater temperatures higher than 16 °C over 14 consecutive weeks in average, from July to October (Figure 8). This temperature threshold is favourable for the growth of all the *O.* cf. *siamensis* strains tested in the present study, even if it is under a low growth rate. Thus, local thermal conditions should favour growth of *O.* cf. *siamensis*, but maybe not enough to form large blooms. On the contrary, weekly SST never exceeded 19 °C in the Bay of Brest, so temperature alone may prevent *O.* cf. *ovata* from growing in these coastal waters. In the end, the fact that *Ostreopsis* blooms have not been reported yet further North than Biarritz (France) could be explained by either a strong limitation of population growth by other environmental factors than temperature or simply a lack of monitoring.

4.5. Toxic risk under climate change

Along the French coast of the Mediterranean Sea, the recurrence of high biomass blooms of *O.* cf. *ovata* is known for decades. For managing the associated risk for humans, monitoring programs are conducted every summer (e.g. Drouet *et al.* (2022)). On a long-term point of view, global ocean warming is expected to affect the distribution and phenology of harmful microalgae (Fu *et al.*, 2012; McLeod *et al.*, 2012; Paerl and Paul, 2012), notably benthic species such as *Ostreopsis* sp. (Tester *et al.*, 2020). Drouet *et al.* (2022) analysed the influence of an increase in SST on *O.* cf. *ovata* development in the NW Mediterranean Sea and showed that it may not result in more intense blooms, but could favour earlier ones. The comparison of the theoretical thermal niche (present study) and the realized one (Drouet *et al.*, 2022) confirmed this assumption: other factors than temperature are already strongly limiting growth of *O.* cf. *ovata* populations in these waters under warm conditions (>25 °C).

In the Basque countries of the Atlantic coast, extensive sanitary and ecological risks associated with *Ostreopsis* developments were reported for the first time in 2021, during a summer bloom constituted of a mixture of *O.* cf. *siamensis* and *O.* cf. *ovata* (Chomérat *et al.*, 2022; Paradis *et al.*, 2024). Main sanitary impact occurred in the French coastline, where about 700 people were intoxicated mainly through cutaneous contact and possibly toxin inhalation (Chomérat *et al.*, 2022; Anses, 2023), whereas in the Spanish basque coast more than 150 people were affected (Goñi *et al.*, 2022). In addition, the present study highlighted the ecological risk that *O.* cf. *siamensis* can have on marine species, even if their toxicity does not rely on any known toxin. Waters of the Bay of Biscay are experiencing a long-term warming trend due to climate change (González-Pola, 2005; deCastro *et al.*, 2009; Costoya *et al.*, 2015). Thus, it is crucial to evaluate the potential impact of rising sea temperature on the toxic risk that *Ostreopsis* blooms may create along this Atlantic coastline, either due to a modification of the species geographical repartition or of their biology (growth and toxicity).

In areas where both *Ostreopsis* species are known to coexist, the thermal niches and growth capacities defined in the present study allow for the definition of two temperature thresholds that are crucial for estimating the relative competitiveness between these species. First, under 22 °C, the direct influence of temperature on cell growth favour the one of *O.* cf. *siamensis* to the detriment of *O.* cf. *ovata*; *O.* cf. *ovata* may even not be able to survive under 19 °C. Second, for temperatures higher than 25 °C, it is the reverse: as long as temperature is the main driving factor for *Ostreopsis* population growth, *O.* cf. *ovata* may strongly overcome *O.* cf. *siamensis*. Thus, every increase in temperature over 19 °C makes temperature more and more favourable to the biomass production of the more toxic species for human health, *O.* cf. *ovata*, to the detriment of the allelopathic *O.* cf. *siamensis*. In terms of toxicity per cell,

biotests conducted in the present study showed that, as long as temperature is below the optimal one (respectively 22 °C for *O.* cf. *siamensis* and 27-28 °C for *O.* cf. *ovata*), any increase in temperature may reduce the toxic effect of *Ostreopsis* cells on some marine organisms. However, toxins dangerous for human health may not follow this trend as, according to Gémin *et al.* (2021), a higher toxin content may be observed for *O.* cf. *ovata* cells growing under sub-optimal temperatures. Under rising temperatures, the evaluation of the toxic risk linked to *Ostreopsis* blooms in Basque countries will have to integrate all these variations in toxicity per cell at the scale of the biomass produced, which is a highly complex task for mixed assemblages.

Out of the coastal zone known for recurrent observations of *Ostreopsis* cells (North from Biarritz, France), *O.* cf. *siamensis* presence was reported in Drouet *et al.* (2021) for several sites all along the Bay of Biscay. In these areas, temperature is still one of the main driver limiting growth and development of *Ostreospsis*. Thus, warming temperatures may increase the risk area by helping for the development of *Ostreopsis* in zones where no bloom has been reported yet. This might be facilitated by water circulation that can allow for cell transfer from well-established populations to less suitable areas (Drouet *et al.*, 2021). In the end, the overall warming of the bay could induce an enlargement of the *Ostreopsis* (both *O.* cf. *siamensis* and *O.* cf. *ovata*) distribution area, increasing the risk in terms of number of impacted coastal zones.

5. Conclusion

Temperature is a key factor controlling microalgae development. In this study, the effect of temperature on growth, toxicity and acclimation indicators was assessed for several strains of *O.* cf. *siamensis* from the Bay of Biscay, NE Atlantic, and *O.* cf. *ovata* from NW Mediterranean Sea. The acclimation of a relatively large number of strains allowed for determining the temperature niche for each species in their respective study site. The niche of *O.* cf. *siamensis* appeared shorter and colder than the one of *O.* cf. *ovata*. *O.* cf. *siamensis* was also characterized by a strain-specific velocity strategy for growth, making some clones able to grow as fast as every competitors do. Pools of pigments and lipids revealed some aspects of thermal acclimation processes in *Ostreopsis* cells. Specific capacities of *O.* cf. *siamensis* to cope with stress of cold temperatures were linked with the activation of xanthophyll cycles in particular. In terms of toxicity, a strong lethal effect was characterized on *Artemia franciscana* that was mainly dependent on currently unknown compounds. This effect decreased for both

species when temperature dropped under the optimal ones. This work suggests strong potential impacts of climate change on the toxic risk associated with *Ostreopsis* blooms, either linked to the species geographic distribution, their growth abilities (playing on biomass production) or their toxicity. In the Bay of Biscay in particular, where mixed assemblages of *O.* cf. *siamensis* and *O.* cf. *ovata* are reported, more investigations are required for forecasting changes in toxic risk in response to environmental forcing. Apart from long-term acclimation to a specific parameter, further studies have to be conducted for better understanding the environmental control of *Ostreopsis* blooms in tidal environments, such as coastal waters of the Bay of Biscay. This should include a focus on strong diel variations of factors, among which temperature or turbulence will be of particular interest.

Acknowledgement

This work was carried out in the frame the PhD thesis of KD, supported by the project CoCliME which is part of ERA4CS, an ERA-NET initiated by JPI Climate, and funded by EPA (IE), ANR (FR), BMBF (DE), UEFISCDI (RO), RCN (NO) and FORMAS (SE), with co-funding by the European Union (Grant 690462). French authors are part of GDR PHYCOTOX, a CNRS/IFREMER network on HAB. We are thankful to Florence Sanchez for her help in sampling *O.* cf. *siamensis* strains in Saint-Jean-de Luz, Gwendoline Heude for her help assisting the analysis of toxicity data, Pascale Malestroit, Marie Latimier and Julien Quéré for their support during the experiment. We are also grateful to the MCCV Strain collection and the EMBRC-France (http://www.embrc-france.fr) for providing us *O.* cf. *ovata* strains from Rochambeau, the SOMLIT ("Service d'Observation en Milieu LITtoral") program from the INSU/CNRS (http://somlit.fr), the Aquarium of San Sebastian for providing us SST dataset in Brest and San Sebastian, and the Ifremer Port-en-Bessin for the analyses of pigment samples. We address our sincere gratitude to the reviewers who accepted to review this manuscript and who helped to its improving. All co-authors have no conflict of interest for the material published.

Authors' contribution

K.D., C.J., R.S. and R.L. designed the experimental protocol. A.L-M. and S.S.P. sampled and isolated *O.* cf. *siamensis* strains from Spanish sites. K.D., C.J. and E.G. conducted the acclimation experiment. M.B. conducted the lipid analyses. D.R. and F.H. conducted the toxin profile analyses. S.S. coordinated the pigment analyses. K.D. and C.J. analysed the results,

prepared the figures and wrote most of the manuscript. R.S, R.L, D.R, F.H., A.L-M. and S.S.P had a significant contribution to the writing of the manuscript. All authors reviewed and accepted the final version of the manuscript.

Figure captions

Figure 1: Map of isolation sites for strains of *Ostreopsis* cf. *siamensis* (blue circles) and *Ostreopsis* cf. *ovata* (orange circle) used in this study.

Figure 2: Maximal growth rates of *O.* cf. *siamensis* (blue) and *O.* cf. *ovata* (orange) at 22 °C for strains isolated from six sampling sites. Black dots represent the average μ_{max} of each strain obtained from three to four replicated estimations. Bars not sharing similar letters indicate a significant difference (Dunn's test, $p < 0.05$) for the dataset pooling three to four strain-specific μ_{max} per site.

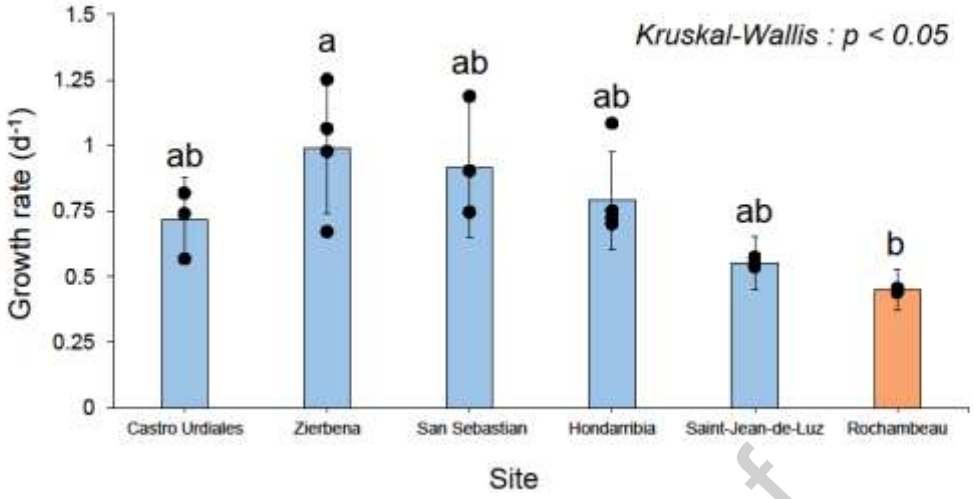

Figure 3: Growth rates of (A) *O.* cf. *siamensis* and (B) *O.* cf. *ovata* as a function of temperature. The black line represents the non-linear exponential product function describing the growth response. The optimal growth temperatures described by the exponential product model are indicated by dashed arrows. Different letters are specifying significant differences (Wilcoxon signed-rank test, $p < 0.05$) between mean growth rates of the pooled strains of *O.* cf. *siamensis* (n=9) or *O.* cf. *ovata* (n=3).

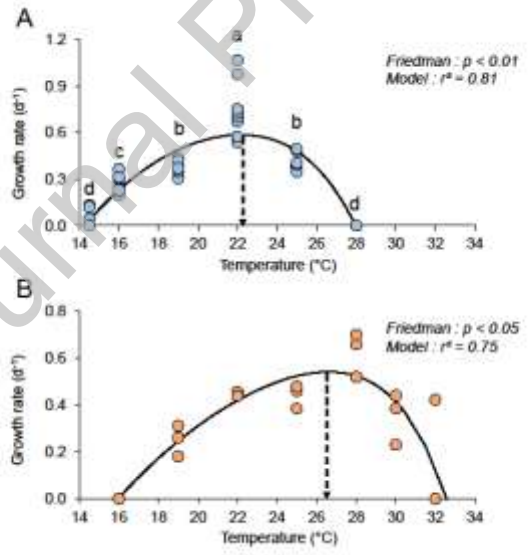

Figure 4: LC_{30} and LT_{30} values after 48 h of exposure of *A. franciscana* nauplii to *Ostreopsis* cf. *siamensis* (A and B) and *Ostreopsis* cf. *ovata* (C and D) strains under various temperature conditions. Hashed bars represent the conditions where the toxicity experiment was assessed only on one strain. Letters indicate a significant difference (Wilcoxon signed-rank, $p < 0.05$) between means of groups.

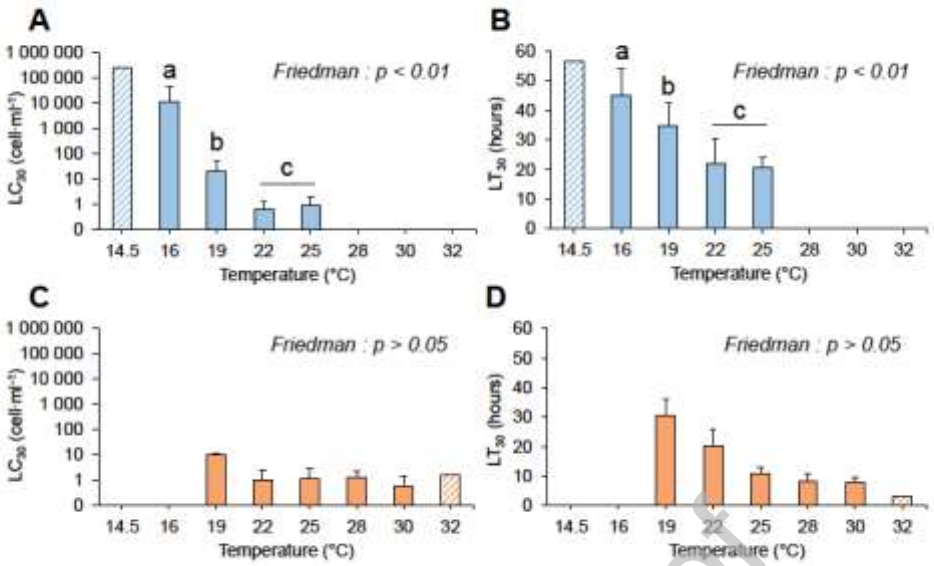

Table 1: Pigment profiles of *O.* cf. *siamensis* and *O.* cf. *ovata* during the thermal acclimation experiment. Pigments were either not detected (dashes), occasionally detected (empty circles) or always detected (black filled circles).

	Pigment	***O.* cf. *siamensis***	***O.* cf. *ovata***
Chlorophylls	Chlorophyll *a*	●	●
	Chlorophyll *b*	○	-
	Chlorophyll *c2*	●	●
	Chlorophyll *c3*	-	-
	Chlorophyllide *a*	-	-
	Chlorophyllide *b*	-	-
	Pheophytin *a*	●	●
	Pheophorbide *a*	-	-
Carotenoids	Alloxanthin	○	●
	Antheraxanthin	○	○
	Astaxanthin	○	●
	β,β-carotene	●	●
	Canthaxanthin	-	-
	Diadinoxanthin	●	●

Diatoxanthin	●	●
Dinoxanthin	-	-
Fucoxanthin	-	-
19'-Butanoyloxyfucoxanthin	-	-
19'-Hexanoyloxyfucoxanthin	-	-
Lutein	●	○
Neoxanthin	-	-
Peridinin	●	●
Prasinoxanthin	-	-
Violaxanthin	○	●
Zeaxanthin	○	○

Figure 5: Chl *a* normalized xanthophyll cycle pigment ratios and de-epoxydized state (DES) in (A, C) *O.* cf. *siamensis* and (B, D) *O.* cf. *ovata* across the temperature acclimation gradient. Filled symbols correspond to average and standard deviation values compiled from nine strains of *O.* cf. *siamensis* (A) and three strains of *O.* cf. *ovata* (B). Empty symbols represent average data obtained from only two *O.* cf. *siamensis* strains (Z8 and SJL1).

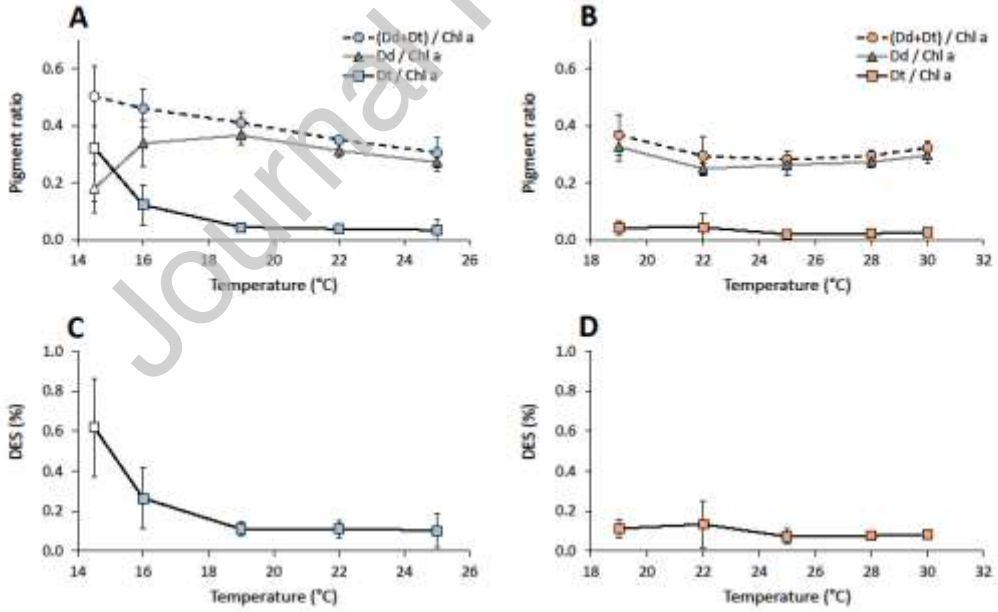

Figure 6: Lipid class concentrations per cell and proportions in (A, C) *O.* cf. *siamensis* and (B, D) *O.* cf. *ovata*. Hatched bars (A, C) represent the concentrations and proportions of lipid classes at 14.5 °C where lipid concentrations of only one *O.* cf. *siamensis* strain (Z8) could be measured.

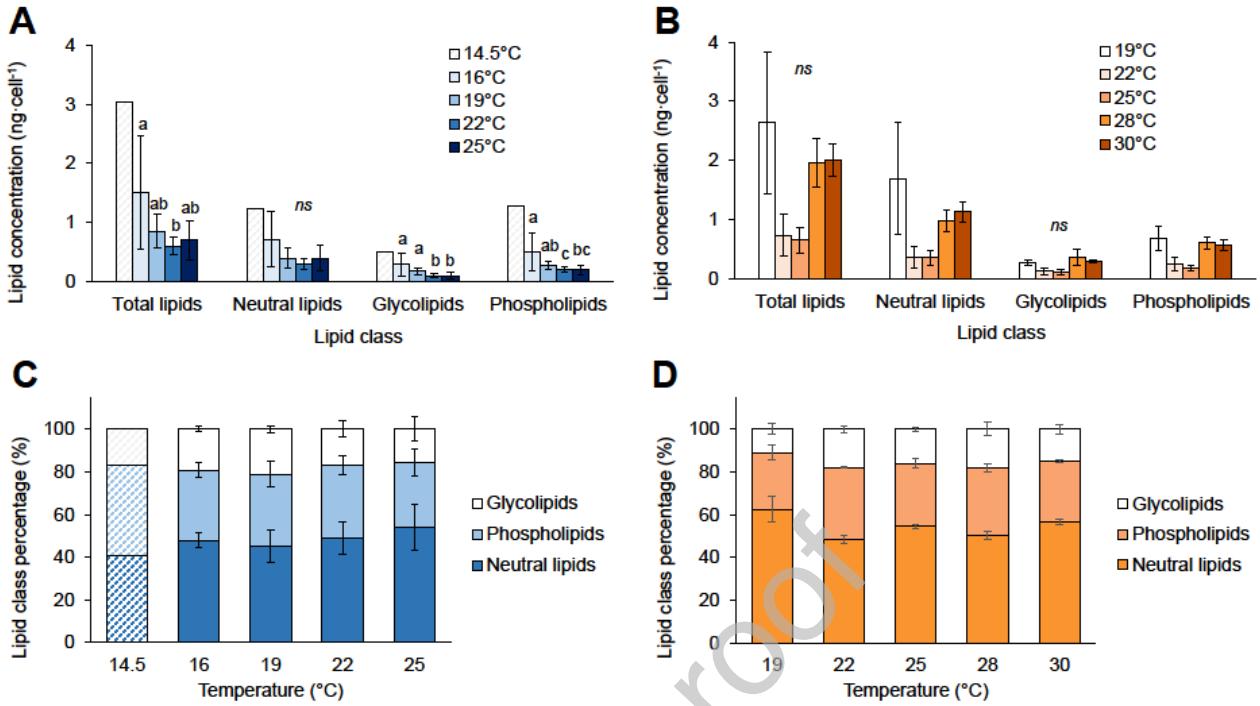

Figure 7: Biplot representations of physiological parameters and individuals on the first two axis of the Principal Component Analysis (PCA) for (A) *O.* cf. *siamensis* and (B) for *O.* cf. *ovata*. Mean values of variables used to create the factorial space (μ_{max}, LC 30, LT 30, concentrations of neutral lipids "NL", glycolipids "GL" and phospholipids "PL" and (Dd+Dt)/Chl *a* and DES ratios) are represented by solid arrows. Convex hulls represent clusters of individuals grouped by temperatures (illustrative variable), with larger dots representing their centroids.

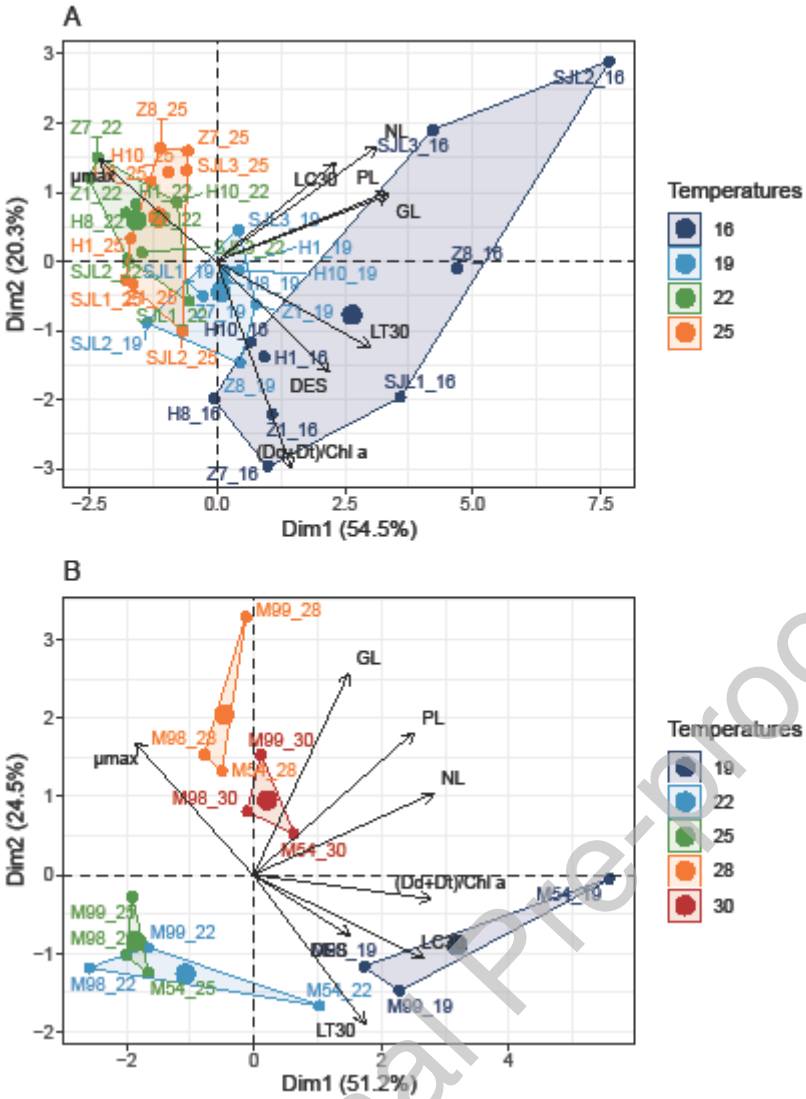

Figure 8: Weekly average of coastal SST in Brest and San Sebastian over the 2000 – 2019 period according to data provided by the SOMLIT and the Aquarium of San Sebastian, respectively.

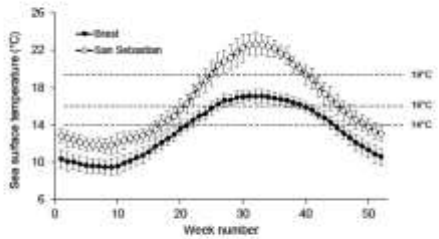

Bibliography

Accoroni, S., Romagnoli, T., Pichierri, S., Totti, C., 2014. New insights on the life cycle stages of the toxic benthic dinoflagellate *Ostreopsis* cf. *ovata*. Harmful Algae 34, 7–16. https://doi.org/10.1016/j.hal.2014.02.003

Accoroni, S., Totti, C., 2016. The toxic benthic dinoflagellates of the genus *Ostreopsis* in temperate areas: a review. Advances in Oceanography and Limnology 7, 1–15. https://doi.org/10.4081/aiol.2016.5591

Anderson, D.M., 2009. Approaches to monitoring, control and management of harmful algal blooms (HABs). Ocean & Coastal Management 52, 342–347. https://doi.org/10.1016/j.ocecoaman.2009.04.006

Anning, T., Harris, G., Geider, R., 2001. Thermal acclimation in the marine diatom *Chaetoceros calcitrans* (Bacillariophyceae). European Journal of Phycology 36, 233–241. https://doi.org/10.1080/09670260110001735388

Anses, 2023. Avis de l'Anses relatif aux risques pour la santé humaine liés aux proliférations d'*Ostreopsis* spp. sur le littoral basque. Saisine n°2021-SA-0212, Anses. 2023, 40 p. ⟨anses-04169914⟩.

Bailleul, B., Rogato, A., De Martino, A., Coesel, S., Cardol, P., Bowler, C., Falciatore, A., Finazzi, G., 2010. An atypical member of the light-harvesting complex stress-related protein family modulates diatom responses to light. Proc. Natl. Acad. Sci. U.S.A. 107, 18214–18219. https://doi.org/10.1073/pnas.1007703107

Behrenfeld, M.J., O'Malley, R.T., Siegel, D.A., McClain, C.R., Sarmiento, J.L., Feldman, G.C., Milligan, A.J., Falkowski, P.G., Letelier, R.M., Boss, E.S., 2006. Climate-driven trends in contemporary ocean productivity. Nature 444, 752–755. https://doi.org/10.1038/nature05317

Ben-Gharbia, H., Yahia, O., Amzil, Z., Chomérat, N., Abadie, E., Masseret, E., Sibat, M., Zmerli Triki, H., Nouri, H., Laabir, M., 2016. Toxicity and Growth Assessments of Three Thermophilic Benthic Dinoflagellates (*Ostreopsis* cf. *ovata*, *Prorocentrum lima* and *Coolia monotis*) Developing in the Southern Mediterranean Basin. Toxins 8, 297. https://doi.org/10.3390/toxins8100297

Berdalet, E., Fleming, L.E., Gowen, R., Davidson, K., Hess, P., Backer, L.C., Moore, S.K., Hoagland, P., Enevoldsen, H., 2016. Marine harmful algal blooms, human health and wellbeing: challenges and opportunities in the 21st century. Journal of the Marine Biological Association of the United Kingdom 96, 61–91. https://doi.org/10.1017/S0025315415001733

Berdalet, E., Tester, P., Chinain, M., Fraga, S., Lemée, R., Litaker, W., Penna, A., Usup, G., Vila, M., Zingone, A., 2017. Harmful Algal Blooms in Benthic Systems: Recent Progress and Future Research. Oceanography 30, 36–45. https://doi.org/10.5670/oceanog.2017.108

Bernard, O., Rémond, B., 2012. Validation of a simple model accounting for light and temperature effect on microalgal growth. Bioresource Technology 123, 520–527. https://doi.org/10.1016/j.biortech.2012.07.022

Berne, N., Fabryova, T., Istaz, B., Cardol, P., Bailleul, B., 2018. The peculiar NPQ regulation in the stramenopile *Phaeomonas* sp. challenges the xanthophyll cycle dogma. Biochimica et Biophysica Acta (BBA) - Bioenergetics 1859, 491–500. https://doi.org/10.1016/j.bbabio.2018.03.013

Blanfuné, A., Boudouresque, C.F., Grossel, H., Thibaut, T., 2015. Distribution and abundance of *Ostreopsis* spp. and associated species (Dinophyceae) in the northwestern Mediterranean: the region and the macroalgal substrate matter. Environmental Science and Pollution Research 22, 12332–12346. https://doi.org/10.1007/s11356-015-4525-4

Bligh, E.G., Dyer, W.J., 1959. A rapid method of total lipid extraction and purification. Can. J. Biochem. Physiol. 37, 911–917. https://doi.org/10.1139/o59-099

Borowitzka, M.A., 2018. The 'stress' concept in microalgal biology—homeostasis, acclimation and adaptation. J Appl Phycol 30, 2815–2825. https://doi.org/10.1007/s10811-018-1399-0

Bravo, I., Anderson, D.M., 1994. The effects of temperature, growth medium and darkness on excystment and growth of the toxic dinoflagellate *Gymnodinium catenatum* from northwest Spain. J Plankton Res 16, 513–525. https://doi.org/10.1093/plankt/16.5.513

Bravo, I., Vila, M., Casabianca, S., Rodriguez, F., Rial, P., Riobó, P., Penna, A., 2012. Life cycle stages of the benthic palytoxin-producing dinoflagellate *Ostreopsis* cf. *ovata* (Dinophyceae). Harmful Algae 18, 24–34. https://doi.org/10.1016/j.hal.2012.04.001

Brissard, C., Herrenknecht, C., Séchet, V., Hervé, F., Pisapia, F., Harcouet, J., Lémée, R., Chomérat, N., Hess, P., Amzil, Z., 2014. Complex Toxin Profile of French Mediterranean *Ostreopsis* cf. *ovata* Strains, Seafood Accumulation and Ovatoxins Prepurification. Marine Drugs 12, 2851–2876. https://doi.org/10.3390/md12052851

Cagide, E., Louzao, M.C., Espiña, B., Vieytes, M.R., Jaen, D., Maman, L., Yasumoto, T., Botana, L.M., 2009. Production of Functionally Active Palytoxin-like Compounds by Mediterranean *Ostreopsis cf. siamensis*. Cell Physiol Biochem 23, 431–440. https://doi.org/10.1159/000218190

Carnicer, O., García-Altares, M., Andree, K.B., Tartaglione, L., Dell'Aversano, C., Ciminiello, P., de la Iglesia, P., Diogène, J., Fernández-Tejedor, M., 2016. *Ostreopsis* cf. *ovata* from western Mediterranean Sea: Physiological responses under different temperature and salinity conditions. Harmful Algae 57, 98–108. https://doi.org/10.1016/j.hal.2016.06.002

Carnicer, O., Guallar, C., Andree, K.B., Diogène, J., Fernández-Tejedor, M., 2015. *Ostreopsis* cf. *ovata* dynamics in the NW Mediterranean Sea in relation to biotic and abiotic factors. Environmental Research 143, 89–99. https://doi.org/10.1016/j.envres.2015.08.023

Chomérat, N., Antajan, E., Auby, I., Bilien, G., Carpentier, L., Casamajor, M.-N. de, Ganthy, F., Hervé, F., Labadie, M., Méteigner, C., Paradis, C., Perrière-Rumèbe, M., Sanchez, F., Séchet, V., Amzil, Z., 2022. First Characterization of *Ostreopsis* cf. *ovata* (Dinophyceae) and Detection of Ovatoxins during a Multispecific and Toxic *Ostreopsis* Bloom on French Atlantic Coast. Marine Drugs 20, 461. https://doi.org/10.3390/md20070461

Chomérat, N., Bilien, G., Derrien, A., Henry, K., Ung, A., Viallon, J., Darius, H.T., Mahana iti Gatti, C., Roué, M., Hervé, F., Réveillon, D., Amzil, Z., Chinain, M., 2019. *Ostreopsis lenticularis* Y. Fukuyo (Dinophyceae, Gonyaulacales) from French Polynesia (South Pacific Ocean): A revisit of its morphology, molecular phylogeny and toxicity. Harmful Algae 84, 95–111. https://doi.org/10.1016/j.hal.2019.02.004

Chomérat, N., Bilien, G., Viallon, J., Hervé, F., Réveillon, D., Henry, K., Zubia, M., Vieira, C., Ung, A., Gatti, C.M. iti, Roué, M., Derrien, A., Amzil, Z., Darius, H.T., Chinain, M., 2020. Taxonomy and toxicity of a bloom-forming *Ostreopsis* species (Dinophyceae, Gonyaulacales) in Tahiti island (South Pacific Ocean): one step further towards resolving the identity of *O. siamensis*. Harmful Algae 98, 101888. https://doi.org/10.1016/j.hal.2020.101888

Ciminiello, P., Dell'Aversano, C., Dello Iacovo, E., Fattorusso, E., Forino, M., Grauso, L., Tartaglione, L., Guerrini, F., Pezzolesi, L., Pistocchi, R., Vanucci, S., 2012. Isolation and Structure Elucidation of Ovatoxin-a, the Major Toxin Produced by *Ostreopsis ovata*. J. Am. Chem. Soc. 134, 1869–1875. https://doi.org/10.1021/ja210784u

Ciminiello, P., Dell'Aversano, C., Iacovo, E.D., Fattorusso, E., Forino, M., Grauso, L., Tartaglione, L., Guerrini, F., Pistocchi, R., 2010. Complex palytoxin-like profile of *Ostreopsis ovata*. Identification of four new ovatoxins by high-resolution liquid chromatography/mass spectrometry. Rapid Commun. Mass Spectrom. 24, 2735–2744. https://doi.org/10.1002/rcm.4696

Ciminiello, P., Dell'Aversano, C., Iacovo, E.D., Fattorusso, E., Forino, M., Tartaglione, L., 2011. LC-MS of palytoxin and its analogues: State of the art and future perspectives. Toxicon 57, 376–389. https://doi.org/10.1016/j.toxicon.2010.11.002

Ciminiello, P., Dell'Aversano, C., Iacovo, E.D., Fattorusso, E., Forino, M., Tartaglione, L., Yasumoto, T., Battocchi, C., Giacobbe, M., Amorim, A., Penna, A., 2013. Investigation of toxin profile of

Mediterranean and Atlantic strains of *Ostreopsis* cf. *siamensis* (Dinophyceae) by liquid chromatography–high resolution mass spectrometry. Harmful Algae 23, 19–27. https://doi.org/10.1016/j.hal.2012.12.002

Cirulis, J.T., Scott, J.A., Ross, G.M., 2013. Management of oxidative stress by microalgae. Can. J. Physiol. Pharmacol. 91, 15–21. https://doi.org/10.1139/cjpp-2012-0249

Cohu, S., Thibaut, T., Mangialajo, L., Labat, J.-P., Passafiume, O., Blanfuné, A., Simon, N., Cottalorda, J.-M., Lemée, R., 2011. Occurrence of the toxic dinoflagellate *Ostreopsis* cf. *ovata* in relation with environmental factors in Monaco (NW Mediterranean). Marine Pollution Bulletin 62, 2681–2691. https://doi.org/10.1016/j.marpolbul.2011.09.022

Costoya, X., deCastro, M., Gómez-Gesteira, M., Santos, F., 2015. Changes in sea surface temperature seasonality in the Bay of Biscay over the last decades (1982–2014). Journal of Marine Systems 150, 91–101. https://doi.org/10.1016/j.jmarsys.2015.06.002

David, H., Ganzedo, U., Laza-Martínez, A., Orive, E., 2012. Relationships between the Presence of *Ostreopsis* (Dinophyceae) in the Atlantic Coast of the Iberian Peninsula and Sea-Surface Temperature. Cryptogamie, Algologie 33, 199–207. https://doi.org/10.7872/crya.v33.iss2.2011.199

David, H., Laza-Martínez, A., Miguel, I., Orive, E., 2013. *Ostreopsis* cf. *siamensis* and *Ostreopsis* cf. *ovata* from the Atlantic Iberian Peninsula: Morphological and phylogenetic characterization. Harmful Algae 30, 44–55. https://doi.org/10.1016/j.hal.2013.08.006

Davison, I.R., 1991. Environmental effects on algal photosynthesis: Temperature. Journal of Phycology 27, 2–8. https://doi.org/10.1111/j.0022-3646.1991.00002.x

deCastro, M., Gómez-Gesteira, M., Alvarez, I., Gesteira, J.L.G., 2009. Present warming within the context of cooling–warming cycles observed since 1854 in the Bay of Biscay. Continental Shelf Research 29, 1053–1059. https://doi.org/10.1016/j.csr.2008.11.016

Delebecq, G., Schmidt, S., Ehrhold, A., Latimier, M., Siano, R., 2020. Revival of Ancient Marine Dinoflagellates Using Molecular Biostimulation. J. Phycol. 56, 1077–1089. https://doi.org/10.1111/jpy.13010

Demmig-Adams, B., Adams, W.W., 2006. Photoprotection in an ecological context: the remarkable complexity of thermal energy dissipation. New Phytologist 172, 11–21. https://doi.org/10.1111/j.1469-8137.2006.01835.x

Demmig-Adams, B., Garab, G., Adams Iii, W., Govindjee (Eds.), 2014. Non-Photochemical Quenching and Energy Dissipation in Plants, Algae and Cyanobacteria, Advances in Photosynthesis and Respiration. Springer Netherlands, Dordrecht. https://doi.org/10.1007/978-94-017-9032-1

Dia, A., Guillou, L., Mauger, S., Bigeard, E., Marie, D., Valero, M., Destombe, C., 2014. Spatiotemporal changes in the genetic diversity of harmful algal blooms caused by the toxic dinoflagellate *Alexandrium minutum*. Mol Ecol 23, 549–560. https://doi.org/10.1111/mec.12617

Ding, Y., Bi, R., Sachs, J., Chen, X., Zhang, H., Li, L., Zhao, M., 2019. Lipid biomarker production by marine phytoplankton under different nutrient and temperature regimes. Organic Geochemistry 131, 34–49. https://doi.org/10.1016/j.orggeochem.2019.01.008

Drouet, K., Jauzein, C., Gasparini, S., Pavaux, A.-S., Berdalet, E., Marro, S., Davenet-Sbirrazuoli, V., Siano, R., Lemée, R., 2022. The benthic toxic dinoflagellate *Ostreopsis* cf. *ovata* in the NW Mediterranean Sea: Relationship between sea surface temperature and bloom phenology. Harmful Algae 112, 102184. https://doi.org/10.1016/j.hal.2022.102184

Drouet, K., Jauzein, C., Herviot-Heath, D., Hariri, S., Laza-Martinez, A., Lecadet, C., Plus, M., Seoane, S., Sourisseau, M., Lemée, R., Siano, R., 2021. Current distribution and potential expansion of the harmful benthic dinoflagellate *Ostreopsis* cf. *siamensis* towards the warming waters of the Bay of Biscay, NORTH-EAST Atlantic. Environ Microbiol 1462-2920.15406. https://doi.org/10.1111/1462-2920.15406

Dubinsky, Z., Stambler, N., 2009. Photoacclimation processes in phytoplankton: mechanisms, consequences, and applications. Aquat. Microb. Ecol. 56, 163–176. https://doi.org/10.3354/ame01345

Durando, P., Ansaldi, F., Oreste, P., Moscatelli, P., Marensi, L., Grillo, C., Gasparini, R., Icardi, G., Collaborative Group for the Ligurian Syndromic Algal Surveillance, 2007. *Ostreopsis ovata* and human health: epidemiological and clinical features of respiratory syndrome outbreaks from a two-year syndromic surveillance, 2005-06, in north-west Italy. Euro Surveill. 12, E070607.1.

Faimali, M., Giussani, V., Piazza, V., Garaventa, F., Corrà, C., Asnaghi, V., Privitera, D., Gallus, L., Cattaneo-Vietti, R., Mangialajo, L., Chiantore, M., 2012. Toxic effects of harmful benthic dinoflagellate *Ostreopsis ovata* on invertebrate and vertebrate marine organisms. Marine Environmental Research 76, 97–107. https://doi.org/10.1016/j.marenvres.2011.09.010

Fanesi, A., Wagner, H., Becker, A., Wilhelm, C., 2016. Temperature affects the partitioning of absorbed light energy in freshwater phytoplankton. Freshw Biol 61, 1365–1378. https://doi.org/10.1111/fwb.12777

Fischer, A.D., Brosnahan, M.L., Anderson, D.M., 2018. Quantitative Response of *Alexandrium catenella* Cyst Dormancy to Cold Exposure. Protist 169, 645–661. https://doi.org/10.1016/j.protis.2018.06.001

Fu, F., Tatters, A., Hutchins, D., 2012. Global change and the future of harmful algal blooms in the ocean. Mar. Ecol. Prog. Ser. 470, 207–233. https://doi.org/10.3354/meps10047

Gašparović, B., Godrijan, J., Frka, S., Tomažić, I., Penezić, A., Marić, D., Djakovac, T., Ivančić, I., Paliaga, P., Lyons, D., Precali, R., Tepić, N., 2013. Adaptation of marine plankton to environmental stress by glycolipid accumulation. Marine Environmental Research 92, 120–132. https://doi.org/10.1016/j.marenvres.2013.09.009

Gémin, M.-P., Bertrand, S., Séchet, V., Amzil, Z., Réveillon, D., 2021. Combined effects of temperature and light intensity on growth, metabolome and ovatoxin content of a Mediterranean *Ostreopsis* cf. *ovata* strain. Harmful Algae 106, 102060. https://doi.org/10.1016/j.hal.2021.102060

Giovagnetti, V., Cataldo, M.L., Conversano, F., Brunet, C., 2012. Growth and photophysiological responses of two picoplanktonic *Minutocellus* species, strains RCC967 and RCC703 (Bacillariophyceae). European Journal of Phycology 47, 408–420. https://doi.org/10.1080/09670262.2012.733030

Giussani, V., Sbrana, F., Asnaghi, V., Vassalli, M., Faimali, M., Casabianca, S., Penna, A., Ciminiello, P., Dell'Aversano, C., Tartaglione, L., Mazzeo, A., Chiantore, M., 2015. Active role of the mucilage in the toxicity mechanism of the harmful benthic dinoflagellate *Ostreopsis* cf. *ovata*. Harmful Algae 44, 46–53. https://doi.org/10.1016/j.hal.2015.02.006

Glibert, P.M., Wilkerson, F.P., Dugdale, R.C., Raven, J.A., Dupont, C.L., Leavitt, P.R., Parker, A.E., Burkholder, J.M., Kana, T.M., 2016. Pluses and minuses of ammonium and nitrate uptake and assimilation by phytoplankton and implications for productivity and community composition, with emphasis on nitrogen-enriched conditions: Pluses and minuses of NH4+ *and* NO3−. Limnol. Oceanogr. 61, 165–197. https://doi.org/10.1002/lno.10203

Goñi, O., Goikolea, J., Garcia-Angulo, I., Yarzabal, A., Laza-Martinez, A., 2022. Investigación de la presencia de *Ostreopsis* spp. en las playas de la CAPV tras el bloom producido en las playas de Donostia - San Sebastián. Rev. salud. ambiant. 22, 197.

González-Pola, C., 2005. Intense warming and salinity modification of intermediate water masses in the southeastern corner of the Bay of Biscay for the period 1992–2003. J. Geophys. Res. 110, C05020. https://doi.org/10.1029/2004JC002367

Goss, R., Jakob, T., 2010. Regulation and function of xanthophyll cycle-dependent photoprotection in algae. Photosynth Res 106, 103–122. https://doi.org/10.1007/s11120-010-9536-x

Goss, R., Latowski, D., 2020. Lipid Dependence of Xanthophyll Cycling in Higher Plants and Algae. Front. Plant Sci. 11, 455. https://doi.org/10.3389/fpls.2020.00455

Goss, R., Latowski, D., Grzyb, J., Vieler, A., Lohr, M., Wilhelm, C., Strzalka, K., 2007. Lipid dependence of diadinoxanthin solubilization and de-epoxidation in artificial membrane systems resembling the lipid composition of the natural thylakoid membrane. Biochimica et

Biophysica Acta (BBA) - Biomembranes 1768, 67–75. https://doi.org/10.1016/j.bbamem.2006.06.006

Goss, R., Lepetit, B., 2015. Biodiversity of NPQ. Journal of Plant Physiology 172, 13–32. https://doi.org/10.1016/j.jplph.2014.03.004

Goss, R., Lohr, M., Latowski, D., Grzyb, J., Vieler, A., Wilhelm, C., Strzalka, K., 2005. Role of Hexagonal Structure-Forming Lipids in Diadinoxanthin and Violaxanthin Solubilization and De-Epoxidation. Biochemistry 44, 4028–4036. https://doi.org/10.1021/bi047464k

Guadayol, Ò., Mendonca, T., Segura-Noguera, M., Wright, A.J., Tassieri, M., Humphries, S., 2021. Microrheology reveals microscale viscosity gradients in planktonic systems. Proc. Natl. Acad. Sci. U.S.A. 118, e2011389118. https://doi.org/10.1073/pnas.2011389118

Guerrini, F., Pezzolesi, L., Feller, A., Riccardi, M., Ciminiello, P., Dell'Aversano, C., Tartaglione, L., Iacovo, E.D., Fattorusso, E., Forino, M., Pistocchi, R., 2010. Comparative growth and toxin profile of cultured *Ostreopsis ovata* from the Tyrrhenian and Adriatic Seas. Toxicon 55, 211–220. https://doi.org/10.1016/j.toxicon.2009.07.019

Guschina, I.A., Harwood, J.L., 2009. Algal lipids and effect of the environment on their biochemistry, in: Kainz, M., Brett, M.T., Arts, M.T. (Eds.), Lipids in Aquatic Ecosystems. Springer New York, New York, NY, pp. 1–24. https://doi.org/10.1007/978-0-387-89366-2_1

Harwood, J.L., 1998. Membrane Lipids in Algae, in: Paul-André, S., Norio, M. (Eds.), Lipids in Photosynthesis: Structure, Function and Genetics, Advances in Photosynthesis and Respiration. Kluwer Academic Publishers, Dordrecht, pp. 53–64. https://doi.org/10.1007/0-306-48087-5_3

Illoul, H., Hernández, F.R., Vila, M., Adjas, N., younes, A.A., Bournissa, M., Koroghli, A., Marouf, N., Rabia, S., Ameur, F.L.K., 2012. The Genus *Ostreopsis* along the Algerian Coastal Waters (SW Mediterranean Sea) Associated with a Human Respiratory Intoxication Episode. Cryptogamie, Algologie 33, 209–216. https://doi.org/10.7872/crya.v33.iss2.2011.209

Jauzein, C., Collos, Y., Garcés, E., Vila, M., Maso, M., 2008. Short-term temporal variability of ammonium and urea uptake by *alexandrium catenella* (dinophyta) in cultures [1]. Journal of Phycology 44, 1136–1145. https://doi.org/10.1111/j.1529-8817.2008.00570.x

Jauzein, C., Couet, D., Blasco, T., Lemée, R., 2017. Uptake of dissolved inorganic and organic nitrogen by the benthic toxic dinoflagellate *Ostreopsis* cf. *ovata*. Harmful Algae 65, 9–18. https://doi.org/10.1016/j.hal.2017.04.005

Jauzein, C., Erdner, D.L., 2013. Stress-related Responses in *Alexandrium tamarense* Cells Exposed to Environmental Changes. J. Eukaryot. Microbiol. 60, 526–538. https://doi.org/10.1111/jeu.12065

Jones, M.R., 2007. Lipids in photosynthetic reaction centres: Structural roles and functional holes. Progress in Lipid Research 46, 56–87. https://doi.org/10.1016/j.plipres.2006.06.001

Kamykowski, D., McCollum, S.A., 1986. The temperature acclimatized swimming speed of selected marine dinoflagellates. J Plankton Res 8, 275–287. https://doi.org/10.1093/plankt/8.2.275

Kana, T.M., Geider, R.J., Critchley, C., 1997. Regulation of photosynthetic pigments in micro-algae by multiple environmental factors: a dynamic balance hypothesis. New Phytol 137, 629–638. https://doi.org/10.1046/j.1469-8137.1997.00857.x

Keller, M.D., Selvin, R.C., Claus, W., Guillard, R.R.L., 1987. Media for the culture of oceanic ultraphytoplankton. Journal of Phycology 23, 633–638. https://doi.org/10.1111/j.1529-8817.1987.tb04217.x

Kern, J., Zouni, A., Guskov, A., Krauß, N., 2009. Lipids in the Structure of Photosystem I, Photosystem II and the Cytochrome b 6 f Complex, in: Wada, H., Murata, N. (Eds.), Lipids in Photosynthesis, Advances in Photosynthesis and Respiration. Springer Netherlands, Dordrecht, pp. 203–242. https://doi.org/10.1007/978-90-481-2863-1_10

Kuczynska, P., Jemiola-Rzeminska, M., Strzalka, K., 2015. Photosynthetic Pigments in Diatoms. Marine Drugs 13, 5847–5881. https://doi.org/10.3390/md13095847

Laabir, M., Jauzein, C., Genovesi, B., Masseret, E., Grzebyk, D., Cecchi, P., Vaquer, A., Perrin, Y., Collos, Y., 2011. Influence of temperature, salinity and irradiance on the growth and cell yield

of the harmful red tide dinoflagellate *Alexandrium catenella* colonizing Mediterranean waters. Journal of Plankton Research 33, 1550–1563. https://doi.org/10.1093/plankt/fbr050

Lacour, T., Babin, M., Lavaud, J., 2020. Diversity in Xanthophyll Cycle Pigments Content and Related Nonphotochemical Quenching (NPQ) Among Microalgae: Implications for Growth Strategy and Ecology. J. Phycol. 56, 245–263. https://doi.org/10.1111/jpy.12944

Lacour, T., Larivière, J., Ferland, J., Bruyant, F., Lavaud, J., Babin, M., 2018. The Role of Sustained Photoprotective Non-photochemical Quenching in Low Temperature and High Light Acclimation in the Bloom-Forming Arctic Diatom *Thalassiosira gravida*. Front. Mar. Sci. 5, 354. https://doi.org/10.3389/fmars.2018.00354

Lacour, T., Larivière, J., Ferland, J., Morin, P.-I., Grondin, P.-L., Donaher, N., Cockshutt, A., Campbell, D.A., Babin, M., 2022. Photoacclimation of the polar diatom *Chaetoceros neogracilis* at low temperature. PLoS ONE 17, e0272822. https://doi.org/10.1371/journal.pone.0272822

Latowski, D., Åkerlund, H.-E., Strzałka, K., 2004. Violaxanthin De-Epoxidase, the Xanthophyll Cycle Enzyme, Requires Lipid Inverted Hexagonal Structures for Its Activity. Biochemistry 43, 4417–4420. https://doi.org/10.1021/bi049652g

Latowski, D., Kuczyńska, P., Strzałka, K., 2011. Xanthophyll cycle – a mechanism protecting plants against oxidative stress. Redox Report 16, 78–90. https://doi.org/10.1179/174329211X13020951739938

Lavaud, J., Goss, R., 2014. The Peculiar Features of Non-Photochemical Fluorescence Quenching in Diatoms and Brown Algae, in: Demmig-Adams, B., Garab, G., Adams Iii, W., Govindjee (Eds.), Non-Photochemical Quenching and Energy Dissipation in Plants, Algae and Cyanobacteria, Advances in Photosynthesis and Respiration. Springer Netherlands, Dordrecht, pp. 421–443. https://doi.org/10.1007/978-94-017-9032-1_20

Lavaud, J., Strzepek, R.F., Kroth, P.G., 2007. Photoprotection capacity differs among diatoms: Possible consequences on the spatial distribution of diatoms related to fluctuations in the underwater light climate. Limnol. Oceanogr. 52, 1188–1194. https://doi.org/10.4319/lo.2007.52.3.1188

Laviale, M., Barnett, A., Ezequiel, J., Lepetit, B., Frankenbach, S., Méléder, V., Serôdio, J., Lavaud, J., 2015. Response of intertidal benthic microalgal biofilms to a coupled light-temperature stress: evidence for latitudinal adaptation along the Atlantic coast of Southern Europe: Microphytobenthos response to light-temperature stress. Environ Microbiol 17, 3662–3677. https://doi.org/10.1111/1462-2920.12728

Laza-Martinez, A., Orive, E., Miguel, I., 2011. Morphological and genetic characterization of benthic dinoflagellates of the genera *Coolia* , *Ostreopsis* and *Prorocentrum* from the south-eastern Bay of Biscay. European Journal of Phycology 46, 45–65. https://doi.org/10.1080/09670262.2010.550387

Lepetit, B., Goss, R., Jakob, T., Wilhelm, C., 2012. Molecular dynamics of the diatom thylakoid membrane under different light conditions. Photosynth Res 111, 245–257. https://doi.org/10.1007/s11120-011-9633-5

Lesser, M.P., 2006. Oxydative stress in marine environments: Biochemistry and Physiological Ecology. Annu. Rev. Physiol. 68, 253–278. https://doi.org/10.1146/annurev.physiol.68.040104.110001

Litchman, E., Klausmeier, C.A., Schofield, O.M., Falkowski, P.G., 2007. The role of functional traits and trade-offs in structuring phytoplankton communities: scaling from cellular to ecosystem level. Ecol Letters 10, 1170–1181. https://doi.org/10.1111/j.1461-0248.2007.01117.x

López-Rosales, L., Gallardo-Rodríguez, J., Sánchez-Mirón, A., Cerón-García, M., Belarbi, E., García-Camacho, F., Molina-Grima, E., 2014. Simultaneous Effect of Temperature and Irradiance on Growth and Okadaic Acid Production from the Marine Dinoflagellate *Prorocentrum belizeanum*. Toxins 6, 229–253. https://doi.org/10.3390/toxins6010229

Mangialajo, L., Ganzin, N., Accoroni, S., Asnaghi, V., Blanfuné, A., Cabrini, M., Cattaneo-Vietti, R., Chavanon, F., Chiantore, M., Cohu, S., Costa, E., Fornasaro, D., Grossel, H., Marco-Miralles, F., Masó, M., Reñé, A., Rossi, A.M., Sala, M.M., Thibaut, T., Totti, C., Vila, M., Lemée, R., 2011. Trends in *Ostreopsis* proliferation along the Northern Mediterranean coasts. Toxicon 57, 408–420. https://doi.org/10.1016/j.toxicon.2010.11.019

Mantoura, R.F.C., Llewellyn, C.A., 1983. The rapid determination of algal chlorophyll and carotenoid pigments and their breakdown products in natural waters by reverse-phase high-performance liquid chromatography. Analytica Chimica Acta 151, 297–314. https://doi.org/10.1016/S0003-2670(00)80092-6

McLeod, D.J., Hallegraeff, G.M., Hosie, G.W., Richardson, A.J., 2012. Climate-driven range expansion of the red-tide dinoflagellate *Noctiluca scintillans* into the Southern Ocean. Journal of Plankton Research 34, 332–337. https://doi.org/10.1093/plankt/fbr112

Medina-Pérez, N.I., Cerdán-García, E., Rubió, F., Viure, L., Estrada, M., Moyano, E., Berdalet, E., 2023. Progress on the Link between Nutrient Availability and Toxin Production by *Ostreopsis* cf. *ovata*: Field and Laboratory Experiments. Toxins 15, 188. https://doi.org/10.3390/toxins15030188

Mizusawa, N., Sakata, S., Sakurai, I., Sato, N., Wada, H., 2009. Involvement of digalactosyldiacylglycerol in cellular thermotolerance in *Synechocystis* sp. PCC 6803. Arch Microbiol 191, 595–601. https://doi.org/10.1007/s00203-009-0486-7

Mock, T., Hoch, N., 2005. Long-Term Temperature Acclimation of Photosynthesis in Steady-State Cultures of the Polar Diatom *Fragilariopsis cylindrus*. Photosynth Res 85, 307–317. https://doi.org/10.1007/s11120-005-5668-9

Morán, X.A.G., López-Urrutia, Á., Calvo-Díaz, A., Li, W.K.W., 2010. Increasing importance of small phytoplankton in a warmer ocean. Global Change Biology 16, 1137–1144. https://doi.org/10.1111/j.1365-2486.2009.01960.x

Morrison, W.R., Smith, L.M., 1964. Preparation of fatty acid methyl esters and dimethylacetals from lipids with boron fluoride–methanol. Journal of Lipid Research 5, 600–608. https://doi.org/10.1016/S0022-2275(20)40190-7

Murata, N., Los, D.A., 1997. Membrane Fluidity and Temperature Perception. Plant Physiology 115, 875–879. https://doi.org/10.1104/pp.115.3.875

Nascimento, S.M., Corrêa, E.V., Menezes, M., Varela, D., Paredes, J., Morris, S., 2012. Growth and toxin profile of *Ostreopsis* cf. *ovata* (Dinophyta) from Rio de Janeiro, Brazil. Harmful Algae 13, 1–9. https://doi.org/10.1016/j.hal.2011.09.008

Novak, T., Godrijan, J., Pfannkuchen, D.M., Djakovac, T., Medić, N., Ivančić, I., Mlakar, M., Gašparović, B., 2019. Global warming and oligotrophication lead to increased lipid production in marine phytoplankton. Science of The Total Environment 668, 171–183. https://doi.org/10.1016/j.scitotenv.2019.02.372

Novak, T., Godrijan, J., Pfannkuchen, D.M., Djakovac, T., Mlakar, M., Baricevic, A., Tanković, M.S., Gašparović, B., 2018. Enhanced dissolved lipid production as a response to the sea surface warming. Journal of Marine Systems 180, 289–298. https://doi.org/10.1016/j.jmarsys.2018.01.006

Nunes, B.S., Carvalho, F.D., Guilhermino, L.M., Van Stappen, G., 2006. Use of the genus *Artemia* in ecotoxicity testing. Environmental Pollution 144, 453–462. https://doi.org/10.1016/j.envpol.2005.12.037

Paerl, H.W., Paul, V.J., 2012. Climate change: Links to global expansion of harmful cyanobacteria. Water Research 46, 1349–1363. https://doi.org/10.1016/j.watres.2011.08.002

Paradis, C., Chomérat, N., Vaucel, J.-A., Antajan, E., Labes, P., Rappoport, M., Labadie, M., 2024. Impacts on Human Health Potentially Caused by Exposure to an Unprecedented *Ostreopsis* spp Bloom in the Bay of Biscay, French Basque Coast. Wilderness & Environmental Medicine 10806032231220405. https://doi.org/10.1177/10806032231220405

Parsons, M.L., Aligizaki, K., Bottein, M.-Y.D., Fraga, S., Morton, S.L., Penna, A., Rhodes, L., 2012. Gambierdiscus and *Ostreopsis*: Reassessment of the state of knowledge of their taxonomy, geography, ecophysiology, and toxicology. Harmful Algae 14, 107–129. https://doi.org/10.1016/j.hal.2011.10.017

Pastor, F., Valiente, J.A., Khodayar, S., 2020. A Warming Mediterranean: 38 Years of Increasing Sea Surface Temperature. Remote Sensing 12, 2687. https://doi.org/10.3390/rs12172687

Pavaux, A.-S., Berdalet, E., Lemée, R., 2020a. Chemical Ecology of the Benthic Dinoflagellate Genus *Ostreopsis*: Review of Progress and Future Directions. Front. Mar. Sci. 7, 498. https://doi.org/10.3389/fmars.2020.00498

Pavaux, A.-S., Rostant, J., Guidi-Guilvard, L.D., Marro, S., Ternon, E., Thomas, O.P., Lemée, R., Gasparini, S., 2019. Effects of the toxic dinoflagellate *Ostreopsis* cf. *ovata* on survival, feeding and reproduction of a phytal harpacticoid copepod. Journal of Experimental Marine Biology and Ecology 516, 103–113. https://doi.org/10.1016/j.jembe.2019.05.004

Pavaux, A.-S., Ternon, E., Dufour, L., Marro, S., Gémin, M.-P., Thomas, O.P., Lemée, R., 2020b. Efficient, fast and inexpensive bioassay to monitor benthic microalgae toxicity: Application to *Ostreopsis* species. Aquatic Toxicology 223, 105485. https://doi.org/10.1016/j.aquatox.2020.105485

Perkins, R.G., Kromkamp, J.C., Serôdio, J., Lavaud, J., Jesus, B., Mouget, J.L., Lefebvre, S., Forster, R.M., 2010. The Application of Variable Chlorophyll Fluorescence to Microphytobenthic Biofilms, in: Suggett, D.J., Prášil, O., Borowitzka, M.A. (Eds.), Chlorophyll a Fluorescence in Aquatic Sciences: Methods and Applications. Springer Netherlands, Dordrecht, pp. 237–275. https://doi.org/10.1007/978-90-481-9268-7_12

Petrou, K., Doblin, M.A., Ralph, P.J., 2011. Heterogeneity in the photoprotective capacity of three Antarctic diatoms during short-term changes in salinity and temperature. Mar Biol 158, 1029–1041. https://doi.org/10.1007/s00227-011-1628-4

Pezzolesi, L., Guerrini, F., Ciminiello, P., Dell'Aversano, C., Iacovo, E.D., Fattorusso, E., Forino, M., Tartaglione, L., Pistocchi, R., 2012. Influence of temperature and salinity on *Ostreopsis* cf. *ovata* growth and evaluation of toxin content through HR LC-MS and biological assays. Water Research 46, 82–92. https://doi.org/10.1016/j.watres.2011.10.029

Pistocchi, R., Pezzolesi, L., Guerrini, F., Vanucci, S., Dell'Aversano, C., Fattorusso, E., 2011. A review on the effects of environmental conditions on growth and toxin production of *Ostreopsis ovata*. Toxicon 57, 421–428. https://doi.org/10.1016/j.toxicon.2010.09.013

Quaas, T., Berteotti, S., Ballottari, M., Flieger, K., Bassi, R., Wilhelm, C., Goss, R., 2015. Non-photochemical quenching and xanthophyll cycle activities in six green algal species suggest mechanistic differences in the process of excess energy dissipation. Journal of Plant Physiology 172, 92–103. https://doi.org/10.1016/j.jplph.2014.07.023

R Core Team, 2023. R: A language and environment for statistical computing. R Foundation for Statistical Computing, Vienna, Austria.

Ras, M., Steyer, J.-P., Bernard, O., 2013. Temperature effect on microalgae: a crucial factor for outdoor production. Rev Environ Sci Biotechnol 12, 153–164. https://doi.org/10.1007/s11157-013-9310-6

Renaud, S.M., Zhou, H.C., Parry, D.L., Thinh, L.-V., Woo, K.C., 1995. Effect of temperature on the growth, total lipid content and fatty acid composition of recently isolated tropical microalgae *Isochrysis* sp., *Nitzschia closterium*, *Nitzschia paleacea*, and commercial species *Isochrysis* sp. (clone T.ISO). J Appl Phycol 7, 595–602. https://doi.org/10.1007/BF00003948

Rhodes, L., 2011. World-wide occurrence of the toxic dinoflagellate genus *Ostreopsis* Schmidt. Toxicon 57, 400–407. https://doi.org/10.1016/j.toxicon.2010.05.010

Sakurai, I., Mizusawa, N., Wada, H., Sato, N., 2007. Digalactosyldiacylglycerol Is Required for Stabilization of the Oxygen-Evolving Complex in Photosystem II. Plant Physiol. 145, 1361–1370. https://doi.org/10.1104/pp.107.106781

Salleh, S., McMinn, A., 2011. The effects of temperature on the photosynthetic parameters and recovery of two temperature benthic microalgae, *Amphora* cf. *coffeaeformis* and *Cocconeis* cf. *sublittoralis* (bacillariophyceae)1: Photosynthesis and temperature stress. Journal of Phycology 47, 1413–1424. https://doi.org/10.1111/j.1529-8817.2011.01079.x

Salvucci, M.E., Crafts-Brandner, S.J., 2004. Inhibition of photosynthesis by heat stress: the activation state of Rubisco as a limiting factor in photosynthesis. Physiol Plant 120, 179–186. https://doi.org/10.1111/j.0031-9317.2004.0173.x

Sarthou, G., Timmermans, K.R., Blain, S., Tréguer, P., 2005. Growth physiology and fate of diatoms in the ocean: a review. Journal of Sea Research 53, 25–42. https://doi.org/10.1016/j.seares.2004.01.007

Scalco, E., Brunet, C., Marino, F., Rossi, R., Soprano, V., Zingone, A., Montresor, M., 2012. Growth and toxicity responses of Mediterranean *Ostreopsis* cf. *ovata* to seasonal irradiance and temperature conditions. Harmful Algae 17, 25–34. https://doi.org/10.1016/j.hal.2012.02.008

Selina, M.S., Morozova, T.V., Vyshkvartsev, D.I., Orlova, T.Yu., 2014. Seasonal dynamics and spatial distribution of epiphytic dinoflagellates in Peter the Great Bay (Sea of Japan) with special emphasis on *Ostreopsis* species. Harmful Algae 32, 1–10. https://doi.org/10.1016/j.hal.2013.11.005

Sepúlveda, J., Cantarero, S.I., 2022. Phytoplankton response to a warming ocean. Science 376, 1378–1379. https://doi.org/10.1126/science.abo5235

Sharma, K.K., Schuhmann, H., Schenk, P.M., 2012. High Lipid Induction in Microalgae for Biodiesel Production. Energies 5, 1532–1553. https://doi.org/10.3390/en5051532

Shears, N.T., Ross, P.M., 2009. Blooms of benthic dinoflagellates of the genus *Ostreopsis*; an increasing and ecologically important phenomenon on temperate reefs in New Zealand and worldwide. Harmful Algae 8, 916–925. https://doi.org/10.1016/j.hal.2009.05.003

Six, C., Sherrard, R., Lionard, M., Roy, S., Campbell, D.A., 2009. Photosystem II and Pigment Dynamics among Ecotypes of the Green Alga *Ostreococcus*. Plant Physiol. 151, 379–390. https://doi.org/10.1104/pp.109.140566

Smayda, T.J., 1997. Harmful algal blooms: Their ecophysiology and general relevance to phytoplankton blooms in the sea. Limnol. Oceanogr. 42, 1137–1153. https://doi.org/10.4319/lo.1997.42.5_part_2.1137

Somerville, C., Browse, J., 1996. Dissecting desaturation: plants prove advantageous. Trends in Cell Biology 6, 148–153. https://doi.org/10.1016/0962-8924(96)10002-7

Stamenković, M., Bischof, K., Hanelt, D., 2014. Xanthophyll Cycle Pool Size and Composition in Several *Cosmarium* Strains (Zygnematophyceae, Streptophyta) are Related to their Geographic Distribution Patterns. Protist 165, 14–30. https://doi.org/10.1016/j.protis.2013.10.002

Sun, X.-M., Ren, L.-J., Zhao, Q.-Y., Ji, X.-J., Huang, H., 2018. Microalgae for the production of lipid and carotenoids: a review with focus on stress regulation and adaptation. Biotechnol Biofuels 11, 272. https://doi.org/10.1186/s13068-018-1275-9

Tanimoto, Y., Yamaguchi, H., Yoshimatsu, T., Sato, S., Adachi, M., 2013. Effects of temperature, salinity and their interaction on growth of toxic *Ostreopsis* sp. 1 and *Ostreopsis* sp. 6 (Dinophyceae) isolated from Japanese coastal waters. Fish Sci 79, 285–291. https://doi.org/10.1007/s12562-013-0597-6

Tawong, W., Yoshimatsu, T., Yamaguchi, H., Adachi, M., 2015. Effects of temperature, salinity and their interaction on growth of benthic dinoflagellates *Ostreopsis* spp. from Thailand. Harmful Algae 44, 37–45. https://doi.org/10.1016/j.hal.2015.02.011

Ternon, E., Pavaux, A.-S., Marro, S., Thomas, O.P., Lemée, R., 2018. Allelopathic interactions between the benthic toxic dinoflagellate *Ostreopsis* cf. *ovata* and a co-occurring diatom. Harmful Algae 75, 35–44. https://doi.org/10.1016/j.hal.2018.04.003

Tester, P.A., Litaker, R.W., Berdalet, E., 2020. Climate change and harmful benthic microalgae. Harmful Algae 91, 101655. https://doi.org/10.1016/j.hal.2019.101655

Thompson, G.A., 1996. Lipids and membrane function in green algae. Biochimica et Biophysica Acta (BBA) - Lipids and Lipid Metabolism 1302, 17–45. https://doi.org/10.1016/0005-2760(96)00045-8

Thompson, P.A., Guo, M., Harrison, P.J., 1992a. Effects of variation in temperature. i. on the biochemical composition of eight species of marine phytoplankton1. J Phycol 28, 481–488. https://doi.org/10.1111/j.0022-3646.1992.00481.x

Thompson, P.A., Guo, M., Harrison, P.J., Whyte, J.N.C., 1992b. Effects of variation in temperature. ii. on the fatty acid composition of eight species of marine phytoplankton1. J Phycol 28, 488–497. https://doi.org/10.1111/j.0022-3646.1992.00488.x

Tian, R.C., 2006. Toward standard parameterizations in marine biological modeling. Ecological Modelling 193, 363–386. https://doi.org/10.1016/j.ecolmodel.2005.09.003

Tichadou, L., Glaizal, M., Armengaud, A., Grossel, H., Lemée, R., Kantin, R., Lasalle, J.-L., Drouet, G., Rambaud, L., Malfait, P., de Haro, L., 2010. Health impact of unicellular algae of the *Ostreopsis* genus blooms in the Mediterranean Sea: experience of the French Mediterranean coast surveillance network from 2006 to 2009. Clinical Toxicology 48, 839–844. https://doi.org/10.3109/15563650.2010.513687

Totti, C., Accoroni, S., Cerino, F., Cucchiari, E., Romagnoli, T., 2010. *Ostreopsis ovata* bloom along the Conero Riviera (northern Adriatic Sea): Relationships with environmental conditions and substrata. Harmful Algae 9, 233–239. https://doi.org/10.1016/j.hal.2009.10.006

Triantaphylidès, C., Havaux, M., 2009. Singlet oxygen in plants: production, detoxification and signaling. Trends in Plant Science 14, 219–228. https://doi.org/10.1016/j.tplants.2009.01.008

Tubaro, A., Durando, P., Del Favero, G., Ansaldi, F., Icardi, G., Deeds, J.R., Sosa, S., 2011. Case definitions for human poisonings postulated to palytoxins exposure. Toxicon 57, 478–495. https://doi.org/10.1016/j.toxicon.2011.01.005

Utermöhl, H., 1958. Zur Vervollkommnung der quantitativen Phytoplankton-Methodik: Mit 1 Tabelle und 15 abbildungen im Text und auf 1 Tafel. SIL Communications, 1953-1996 9, 1–38. https://doi.org/10.1080/05384680.1958.11904091

Van Heukelem, L., Thomas, C.S., 2001. Computer-assisted high-performance liquid chromatography method development with applications to the isolation and analysis of phytoplankton pigments. Journal of Chromatography A 910, 31–49. https://doi.org/10.1016/S0378-4347(00)00603-4

Vanhaecke, P., Persoone, G., Claus, C., Sorgeloos, P., 1981. Proposal for a short-term toxicity test with *Artemia* nauplii. Ecotoxicology and Environmental Safety 5, 382–387. https://doi.org/10.1016/0147-6513(81)90012-9

Verma, A., Hoppenrath, M., Harwood, T., Brett, S., Rhodes, L., Murray, S., 2016. Molecular phylogeny, morphology and toxigenicity of *Ostreopsis* cf. *siamensis* (Dinophyceae) from temperate south-east Australia: Merimbula *Ostreopsis*. Phycological Research 64, 146–159. https://doi.org/10.1111/pre.12128

Verma, A., Hoppenrath, M., Smith, K.F., Murray, J.S., Harwood, D.T., Hosking, J.M., Rongo, T., Rhodes, L.L., Murray, S.A., 2023. *Ostreopsis* Schmidt and *Coolia* Meunier (Dinophyceae, Gonyaulacales) from Cook Islands and Niue (South Pacific Ocean), including description of *Ostreopsis tairoto* sp. nov. Sci Rep 13, 3110. https://doi.org/10.1038/s41598-023-29969-z

Vidyarathna, N., Granéli, E., 2012. Influence of temperature on growth, toxicity and carbohydrate production of a Japanese *Ostreopsis ovata* strain, a toxic-bloom-forming dinoflagellate. Aquatic Microbial Ecology 65, 261–270. https://doi.org/10.3354/ame01555

Vila, M., Abós-Herràndiz, R., Isern-Fontanet, J., Àlvarez, J., Berdalet, E., 2016. Establishing the link between *Ostreopsis* cf.*ovata* blooms and human health impacts using ecology and epidemiology. Scientia Marina 80, 107–115. https://doi.org/10.3989/scimar.04395.08A

Wood, A.M., Everroad, R.C., Wingard, L.M., 2005. Measuring growth rates in microalgal cultures. Algal Culturing Techniques 269–288.

Yamaguchi, H., Yoshimatsu, T., Tanimoto, Y., Sato, S., Nishimura, T., Uehara, K., Adachi, M., 2012. Effects of temperature, salinity and their interaction on growth of the benthic dinoflagellate *Ostreopsis* cf. *ovata* (Dinophyceae) from Japanese coastal waters: Growth features of Japanese *O.* cf. *ovata*. Phycological Research 60, 297–304. https://doi.org/10.1111/j.1440-1835.2012.00660.x

Young, J.N., Goldman, J.A.L., Kranz, S.A., Tortell, P.D., Morel, F.M.M., 2015. Slow carboxylation of R ubisco constrains the rate of carbon fixation during A ntarctic phytoplankton blooms. New Phytol 205, 172–181. https://doi.org/10.1111/nph.13021

Zapata, M., Fraga, S., Rodríguez, F., Garrido, J., 2012. Pigment-based chloroplast types in dinoflagellates. Mar. Ecol. Prog. Ser. 465, 33–52. https://doi.org/10.3354/meps09879

Zuluaga, M., Gueguen, V., Pavon-Djavid, G., Letourneur, D., 2017. Carotenoids from microalgae to block oxidative stress. Bioimpacts 7, 1–3. https://doi.org/10.15171/bi.2017.01

Declaration of interests

☒ The authors declare that they have no known competing financial interests or personal relationships that could have appeared to influence the work reported in this paper.

☐ The authors declare the following financial interests/personal relationships which may be considered as potential competing interests: